Genotype-by-environment Interaction in Holstein Heifer Fertility Traits using Single-step Genomic Reaction Norm Models

Rui Shi
Wageningen University & Research
Luiz Brito
Purdue University West Lafayette
Aoxing Liu
Aarhus University
Hanpeng Luo
China Agricultural University
Ziwei Chen
China Agricultural University
Lin Liu
Beijing Dairy Cattle Center
Gang Guo
Beijing Sunlon Livestock Development Co. Ltd
Herman Mulder
Wageningen University & Research
Bart Ducro
Wageningen University & Research
Aart van der Linden
Wageningen University & Research
Yachun Wang (wangyachun@cau.edu.cn)
China Agricultural University

Research Article

Keywords: heifer, heat stress, genotype by environment interaction, reaction norm, single-step GWAS

Posted Date: December 15th, 2020

DOI: https://doi.org/10.21203/rs.3.rs-124685/v1

Version of Record: A version of this preprint was published on March 17th, 2021. See the published version at https://doi.org/10.1186/s12864-021-07496-3.

Genotype-by-environment interaction in Holstein heifer fertility traits using single-step genomic reaction norm models

Rui Shi[1,2,3], Luiz Fernando Brito[4], Aoxing Liu[1,5], Hanpeng Luo[1], Ziwei Chen[1], Lin Liu[6], Gang Guo[7*], Herman Mulder[2*], Bart Ducro[2], Aart van der Linden[3,8] and Yachun Wang[1*]

[1] Key Laboratory of Animal Genetics, Breeding and Reproduction, MARA, National Engineering Laboratory of Animal Breeding, College of Animal Science and Technology, China Agricultural University, Beijing 100193, China

[2] Animal Breeding and Genomics Group, Wageningen University & Research, P.O. Box 338, 6700 AH Wageningen, the Netherlands

[3] Animal Production System Group, Wageningen University & Research, P.O. Box 338, 6700 AH Wageningen, the Netherlands

[4] Department of Animal Sciences, Purdue University, West Lafayette, Indiana, 47907, USA

[5] Center for Quantitative Genetics and Genomics, Aarhus University, 8830, Tjele, Denmark

[6] Beijing Dairy Cattle Center, Beijing 100192, China

[7] Beijing Sunlon Livestock Development Co. Ltd, Beijing 100176, China

[8] Cooperation CRV, 6800 AL Arnhem, the Netherlands

*** Corresponding author:**

Gang Guo

guogang2180@126.com

Herman Mulder

han.mulder@wur.nl

Yachun Wang

wangyachun@cau.edu.cn

ABSTRACT

Background: The effect of heat stress on livestock production is a worldwide issue, where animal performance is influenced by exposure to high environmental temperatures, indicating the existence of possible genotype-by-environment interactions (G×E). The main objectives of this study were to (1) detect the time periods in which heifer fertility traits are more sensitive to the exposure to high environmental temperature and/or humidity, (2) investigate G×E due to heat stress in heifer fertility traits, and (3) identify genomic regions associated with heifer fertility and heat stress in Holstein cattle.

Results: Phenotypic records for three heifer fertility traits (i.e., age at first calving, interval from first to last service, and conception rate at the first service) were collected, from 2005 to 2018, for 56,998 Holstein heifers raised in 15 herds in the Beijing area (China). By integrating environmental data including hourly air temperature and relative humidity, the critical periods in which the heifers are more sensitive to heat stress were defined as <=30 days before the first service for age at first calving and interval from first to last service, or 10 days before and <= 60 days after

the first service for conception rate. Using reaction norm models, significant G×E was detected for all three traits regarding both environmental gradients, proportion of days exceeding heat threshold and minimum temperature humidity index. Through single-step genome-wide association study, *PLAG1*, *AMHR2*, *SP1*, *KRT8*, *KRT18*, *MLH1*, and *EOMES* were suggested as candidate genes for heifer fertility while *HCRTR1*, *AGRP*, *PC*, and *GUCY1B1* were for heat tolerance.

Conclusions: The critical periods in which reproductive perfromances of heifers are more sensitive to heat stress are trait-dependent. Thus, detailed analysis should be conducted to determine this particular period for other fertility traits. The considerable magnitude of G×E and sire re-ranking indicates the necessity to consider G×E in breeding schemes. This will enable selection of more heat-tolerant animals with high reproductive efficiency under harsh climatic conditions. The candidate genes identified to be linked with response to heat stress provide a better understanding of the underlying biological mechanisms of heat tolerance in dairy cattle.

Keywords: heifer; heat stress; genotype by environment interaction; reaction norm; single-step GWAS

BACKGROUND

In modern dairy cattle, female fertility is of great importance, due to its close relationship with reproductive management, veterinary treatments, involuntary culling and, eventually, the farm profitability [1]. However, as widely emphasized in previous

studies [2–4], the low heritability estimates for fertility traits and unfavorable genetic correlations with milk production traits have led to reduced genetic progress for female fertility traits. Moreover, the increase of joint genetic evaluation across farms in various geographical locations emphasizes the role that genotype by environment interactions (G×E) [5] might play, and consequently, the selection for animals (especially bulls) that have progeny with high performance even in challenging environments. Significant G×E for female fertility traits have been detected in several Holstein populations, where the "E" were the production system and grass ratio of feed [6], and herd reproduction level [7]. However, the investigation for other important environmental variations such as the climatic change remain scarce.

With global warming and climatic change, heat stress has already become an issue for livestock production in many countries around the world [8]. The temperature and humidity index (THI) is often used as an environmental indicator to assess the condition of heat stress in dairy cattle [9]. It is widely accepted that dairy cows start to experience mild heat stress when THI surpasses 72 [10]. Studies of American Holstein population have shown that heat conditions can lead to 165 kg loss of milk yield annually and 0.4% reduce in milk fat percentage [11, 12], 0.85 kg decrease in feed intake with one unit increase in air temperature [13], and about 15% decrease in conception rate when THI surpasses 72 [14].

In summer (from June to August), the average daily THI, in many regions of the world, can exceed 72, indicating that dairy cattle raised in these regions may suffer from mild to severe heat stress [15]. For instance, in Beijing (China), the THI fluctuates

89 substantially within a day, that is, extremely high THI in the afternoon and dramaticly
90 reduces to thermoneutral level in the evening). The difference in hourly THI within a
91 day can be up to 30 THI units during the late summer, but the daily average is usually
92 just relatively “mild” (Suppl. File 1). In such case, simply using the daily average of
93 THI may lead to the underestimation of the impact of heat stress. In addition to the
94 timing of a day, for a dairy cow, the timing of its reproductive period may also influence
95 the response to heat stress. Fertility performance may be compromised when an animal
96 experiences heat stress in certain physiological stages. Several studies have
97 demonstrated that the conception rate of dairy cows decreased when they experienced
98 heat stress before and after insemination [16–18], which emphasized the role of critical
99 periods exposed to heat conditions. To the best of our knowledge, no studies have
100 identified the most influential (critical) period for fertility traits due to their complex
101 characteristics. However, this is of utmost value for incorporating G×E models in
102 genetic and genomic evaluations.

103 Reaction norm models (RNM) are widely used to detect G×E when the
104 differences in environments can be measured by a continuous environmental gradient
105 (EG) [5]. In RNM, the breeding value of an animal is partitioned into an environment-
106 independent part (intercept) and an environment-dependent part (slope). The
107 relationship matrix of the RNM can be structured either by pedigree, i.e. pedigree-based
108 best linear unbiased predictor (BLUP), or combing both pedigree and genomic
109 information, i.e. single-step genomic BLUP (ssGBLUP) [19, 20]. On the basis of
110 ssGBLUP, Wang et al. [21] proposed a method termed single-step GWAS (ssGWAS)

which can obtain marker effects from estimated breeding values. Markers related with the intercept and slope could be mapped by applying ssGWAS procedures using RNMs.

The main objectives of this study were to: (1) explore the most heat-sensitive periods regarding heifer fertility (age at first calving – AFC, interval from first to last service – IFL, and conception rate of first service – CR); (2) detect G×E for heifer fertility traits using RNMs with pedigree-genomic combined relationship matrix; and (3) unravel genomic regions contributing to heat tolerance and heifer fertility traits in high-producing Holstein cattle.

RESULTS

Descriptive statistics

The summary statistics for heifer fertility traits are shown in Table 1. Large phenotypic variation was detected, especially for IFL (coefficient of variation equals to 1.89) and CR (coefficient of variation equals to 0.83). The genetic parameters estimated using the conventional animal model, which were relatively low, are also provided in Table 1.

Table 1 Descriptive statistics of heifer fertility traits and genetic parameters estimated using pedigree-based animal models

Trait[a]	N	Mean	SD	CV	Min	Max	σ_a^2	σ_e^2	h^2
AFC	56998	769.05	74.06	0.10	505	1100	794.40 (54.27)	4035.00 (46.35)	0.16 (0.011)
IFL	56998	29.25	55.17	1.89	0	365	190.42 (22.33)	2740.10 (23.82)	0.06 (0.007)
CR	56998	0.59	0.49	0.83	0	1	6.61e-3 (1.11e-3)	2.16e-1 (1.57e-3)	0.03 (0.005)

[a] AFC = age at first calving, IFL = interval from first to last service, CR = conception rate of first service.

Critical period selection for each environmental gradient scenario

Two heat related EGs were used in the current study: 1) the number of days that exceeded the THI threshold in the evaluated critical period (prop-EG); 2) the minimum THI for each day of the candidate period (mTHI-EG). To avoid the underestimation of the heat stress effect, the days in which the hourly THI was higher than 72 for six continuous hours were considered as heat-stress days for prop-EG. Akaike Information Criteria (AIC) [22] was obtained for various time combinations to select the best fit period for each trait.

The critical periods (Fig. 1) selected for each trait and EG under scenario one (S1) and scenario two (S2) are listed in Table 2. The same 60 days, from 30 days before the first insemination to 30 days after the first insemination, were chosen as the control period for S1. For S2, critical periods ranged from 30 to 70 days, of which only the period (-90, -30) for IFL was the same for both EGs. Only the critical periods of CR end after the first service (60 or 30 days). The detailed results of AICs for the 19 tested combinations are presented in Supp. File 2.

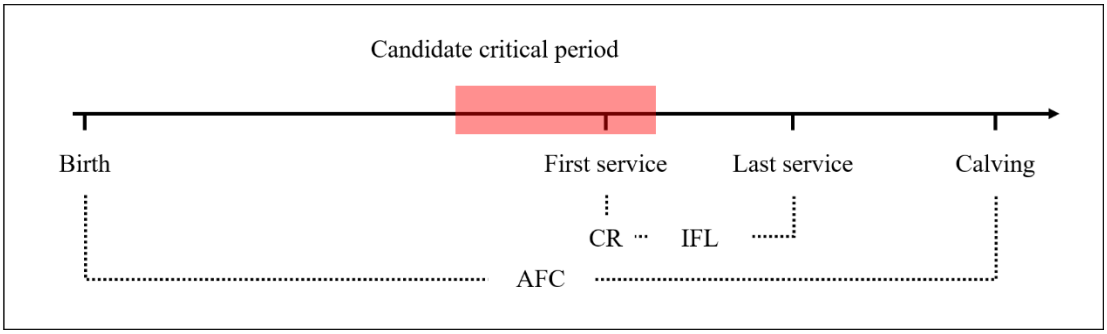

Fig. 1 Reproductive events and the definition of critical period in heifers. The red rectangle represents the critical period, defining as the time period of which heifers are likely to suffer from heat stress. AFC = age at first calving, IFL = interval from first to last service, CR = conception rate of first service.

Table 2 The critical periods selected for each trait in different scenarios

EG[a]	Trait[b]	Scenario[c]	Number of days	Period[d]
Prop-EG	AFC	S1	60	(-30, 30)
		S2	60	(-90, -30)
	IFL	S1	60	(-30, 30)
		S2	60	(-90, -30)
	CR	S1	60	(-30, 30)
		S2	70	(-10, 60)
mTHI-EG	AFC	S1	60	(-30, 30)
		S2	30	(-90, -60)
	IFL	S1	60	(-30, 30)
		S2	60	(-90, -30)
	CR	S1	60	(-30, 30)
		S2	40	(-10, 30)

[a] prop-EG = the number of days that exceeding the threshold temperature humidity index in the period; mTHI-EG = minimum temperature humidity index for each day of the period

[b] AFC = age at first calving; IFL = interval from the first to last service; CR = conception rate of first service

[c] S1 = control critical period; S2 = periods selected based on the Akaike's information criterion

[d] Periods were counted based on the first service day; minus means before and plus means after.

The definitions of two types of EGs had some overlaps. For example, prop-EG would be recorded as 1 if minimum THI of all the days in critical period were above 67.02 (Table 3). To calculate the overlap rate between prop-EG and mTHI-EG, top animals sorted by genomic estimated breeding values (gEBV), with estimation accuracy greater than 0.4 (average accuracy for three traits), were chosen for each trait with regards to each EG. When using the ***H*** matrix, approximately 75% of the heifers were the same in both scenarios for AFC and IFL, but relatively low (29.63% ~ 65.82%) overlap rates were observed in CR (Table 3). Similar results were found when using the ***A*** matrix (Supp. File 3).

Table 3 The proportions of overlapped top 1% heifers[a] from using prop-EG and mTHL-EG as environmental gradients (EGs) by reaction norm models (RNM) with the ***H*** matrix in Holstein cattle.

EG[b]		AFC[c]		IFL		CR	
Prop-EG	mTHI-EG	S1[d]	S2	S1	S2	S1	S2
0.2	43.03	76.47%	82.69%	72.92%	64.37%	29.63%	36.63%
0.4	48.29	84.57%	87.35%	81.24%	77.69%	59.60%	51.50%
0.6	52.34	88.24%	82.02%	85.68%	78.91%	65.82%	60.93%
0.8	55.54	83.02%	75.47%	80.69%	75.47%	65.70%	62.93%
1	67.02	82.24%	76.03%	79.69%	74.92%	64.04%	60.27%

[a] Heifers were selected based on gEBV and accuracy of estimation (> 0.4)

[b] prop-EG = using the number of days that exceeding the threshold temperature humidity index in the period as EG; mTHI-EG = using the minimum temperature humidity index of a day of the critical period as EG

[c] AFC = age at first calving; IFL = interval from the first to last service; CR = conception rate of first service

[d] S1 = reference period; S2 = periods selected based on the Akaike's information criterion

(Co)variance Components and G×E

The estimates of (co)variance components obtained from RNMs with different kinship matrices (***A*** or ***H***) were similar for all traits analyzed. The correlation coefficients between the intercept and slope for each trait were all negative and ranged from -0.25 (IFL in S1 of prop-EG) to -0.98 (CR in both S1 and S2 of mTHI-EG) using the ***H*** matrix (Table 4). Furthermore, the absolute value of coefficients estimated using prop-EG were relatively small than those using mTHI-EG, especially for AFC and IFL. The genetic parameters estimated by ***A*** matrix are shown in Supp. File 4.

Table 4 Variances of the intercept ($\sigma^2_{a_0}$) and slope ($\sigma^2_{a_1}$), the covariance between the intercept and slope ($\sigma_{a_0 a_1}$), residual variance (σ^2_e) and genetic correlation between the intercept and slope ($r_{a_0 a_1}$), with their standard errors in parentheses, estimated using reaction norm models with ***H*** matrix in Holstein cattle.

EG[a]	Trait[b]	Scenario[c]	$\sigma^2_{a_0}$	$\sigma^2_{a_1}$	$\sigma_{a_0 a_1}$	σ^2_e	$r_{a_0 a_1}$

Prop-EG	AFC	S1	971.97 (62.74)	0.53 (0.05)	-9.62 (1.41)	3413.70 (45.80)	-0.43 (0.02)
		S2	963.72 (60.99)	0.96 (0.06)	-14.05 (1.62)	3203.00 (44.60)	-0.46 (0.01)
	IFL	S1	218.16 (26.82)	0.25 (0.03)	-1.80 (0.68)	2456.90 (25.14)	-0.25 (0.03)
		S2	236.35 (27.59)	0.51 (0.03)	-4.98 (0.87)	2323.10 (24.76)	-0.46 (0.02)
	CR	S1	1.01e-2 (1.60e-3)	1.60e-5 (2.00e-6)	-3.35e-4 (5.20e-5)	1.99e-1 (1.61e-03)	-0.83 (0.05)
		S2	1.12e-2 (1.71e-3)	1.30e-5 (2.00e-6)	-3.23e-4 (4.70e-5)	1.98e-1 (1.62e-3)	-0.84 (0.05)
mTHI-EG	AFC	S1	2735.10 (233.57)	1.37 (0.12)	-51.60 (5.10)	3396.80 (45.06)	-0.84 (0.03)
		S2	3950.90 (271.77)	2.06 (0.12)	-81.46 (5.69)	3194.70 (43.73)	-0.90 (0.03)
	IFL	S1	1073.60 (126.34)	0.78 (0.07)	-26.15 (2.92)	2417.70 (25.10)	-0.90 (0.04)
		S2	1591.40 (143.27)	1.24 (0.08)	-41.85 (3.35)	2309.10 (24.37)	-0.94 (0.03)
	CR	S1	7.78e-2 (9.60e-3)	4.30e-5 (5.00e-6)	-1.81e-3 (2.14e-4)	1.99e-1 (1.58e-3)	-0.98 (0.06)
		S2	8.90e-2 (1.03e-2)	4.50e-5 (5.00e-6)	-1.96e-3 (2.19e-4)	1.98e-1 (1.59e-3)	-0.98 (0.05)

[a] prop-EG = the number of days that exceeding the threshold temperature humidity index in the period; mTHI-EG = minimum temperature humidity index for each day of the period

[b] AFC = age at first calving; IFL = interval from the first to last service; CR = conception rate of first service

[c] S1 = reference period; S2 = periods selected based on the Akaike's information criterion

Heritabilities estimated from genomic RNM using prop-EG and mTHI-EG are presented in Fig 2. Generally, AFC had the highest heritability estimates, whereas CR was the least heritable across all EGs. The shapes of heritability curves were similar when using different relationship matrices but different across EGs. The curve patterns were quadratic for mTHI-EG, which indicated that the highest heritabilities were generally observed in either cold (mTHI-EG < 20) or heat-stress environments (mTHI-EG > 72). However, the patterns were flatter when prop-EG was used, and the highest heritabilities only appeared in heat stress conditions. Similar curve patterns were observed when using the ***A*** matrix (Suppl File 5).

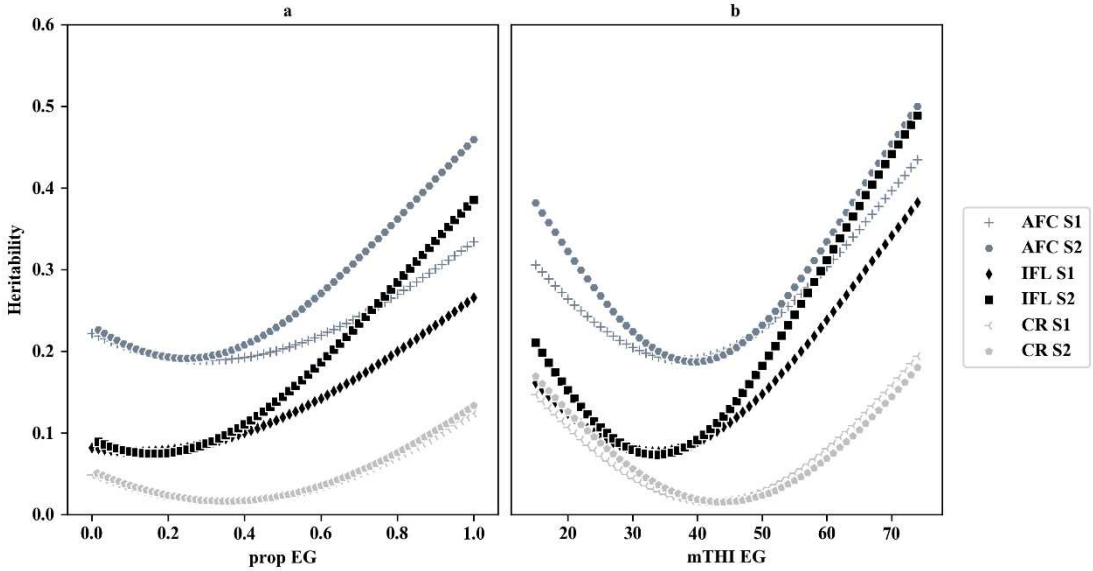

Fig. 2 Heritabilities estimated by reaction norm models with the matrix ***H*** using **a**) prop-EG or **b**) mTHI-EG as environmental gradient. For **a**), the x-axis is the proportion of days exceeding the threshold with a range of 0 to 1; while for **b**), the x-axis is the minimum THI with a range of 15 to 75.

As shown in Table 4, for all traits, the variance of the slope was significantly different from zero based on a one-tailed test ($P < 0.01$), indicating the existence of G×E. Genetic correlations between different EGs, from RNM with the ***H*** matrix, are shown in Fig. 3. Generally, the more different the EGs, the less they were correlated. More negative coefficients of correlation were obtained for AFC and IFL when the mTHI-EG was evaluated, compared with prop-EG. This is consistent with much stronger correlation between the intercept and slope being observed when using mTHI-EG as EG compared to using prop-EG as EG. Similar patterns were also observed when using ***A*** matrix (Suppl File 6).

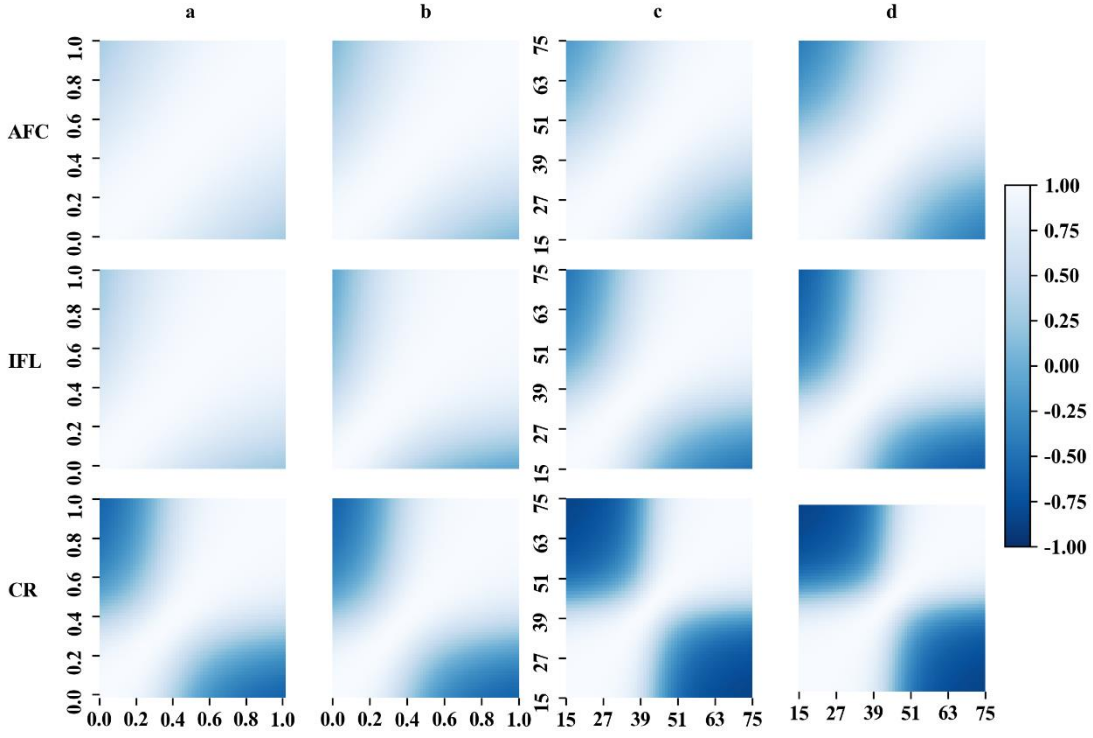

Fig. 3 Genetic correlations estimated by reaction norm models (RNMs) with the matrix ***H***. The color indicates the magnitude of the genetic correlation. **a**) Correlations between different levels of prop-EG estimated from RNM under S1. The x-axis and y-axis are

the proportion of days exceeding the threshold, ranging from 0 to 1. **b**) Correlations between different levels of prop-EG estimated from RNM under S2. The x-axis and y-axis are the proportion of days exceeding the threshold, ranging from 0 to 1. **c**) Correlations between different levels of mTHI-EG estimated from RNM under S1. The x-axis and y-axis are the minimum THI, ranging from 15 to 75. **d**) Correlations between different levels of mTHI-EG estimated from RNM under S2. The x-axis and y-axis are the minimum THI, ranging from 15 to 75.

Among the top sires with more than 20 daughters with phenotypes, the number of sires overlapping across the two EGs, reflecting the magnitude of the re-ranking of sires, are listed in Table 5. The number of overlapped sires decreased as the EGs became more divergent, especially for CR (e.g. from 11 to 1 in S2 of prop-EG). The magnitude of re-ranking increased when using mTHI-EG (only 3 common sires in all environmental combinations).

Table 5 The number of common animals among the top 50 sires between 2 levels of EGs

EG[a]	Trait[b]	Scenario[c]	1 vs. 99%[d]	5 vs. 95%	10 vs. 90%	25 vs. 75%
Prop-EG	AFC	S1	18	20	21	28
		S2	13	14	17	28
	IFL	S1	18	20	21	29
		S2	12	14	17	27
	CR	S1	0	0	1	7
		S2	1	1	3	11
mTHI-EG	AFC	S1	5	8	15	25
		S2	3	4	9	24

	IFL	S1	3	5	6	22
		S2	0	0	2	22
	CR	S1	0	0	0	3
		S2	0	0	0	3

[a] prop-EG = the number of days that exceeding the threshold temperature humidity index in the period; mTHI-EG = minimum temperature humidity index for each day of the period

[b] AFC = age at first calving; IFL = interval from the first to last service; CR = conception rate of first service

[c] S1 = reference period; S2 = periods selected based on the Akaike's information criterion

[d] the number of overlapping animals in the top sires in the 1 and 99%, 5 and 95%, 10 and 90%, and 25 and 75% quantiles of EGs

We further visualized breeding value re-ranking by plotting gEBV of sires with the most preferential intercepts (gEBV less than average minus two times standard deviation for AFC and IFL; gEBV greater than average plus two times standard deviation for CR) in Fig. 4. The top 5 sires with the flattest slopes (more climatic resilient) were drawn in red, while the top 5 sires with the steep slopes (more climatic sensitive) were drawn in blue. In this case, sires that are sensitive to the environments (blue lines), would perform worse than those had flat slopes (red lines) in heat stressed conditions. For instance, the gEBV of CR is 0.10 when prop-EG is 0, but the gEBVs for blue lines decreased to around -0.15 when prop-EG is 1. Meanwhile, the gEBVs of the red lines were stable along the whole prop-EG (Fig. 4a). This further verified the

existence of G×E regarding the change of mTHI-EG and/or prop-EG. Larger changes were observed for gEBVs when using mTHI-EG. Implementing mTHI-EG, gEBVs of IFL for two bulls increased from around -50 day in thermoneutral condition to 0 day in heat stress condition (Fig. 4c-d), which is nearly twice the change as gEBVs using prop-EG.

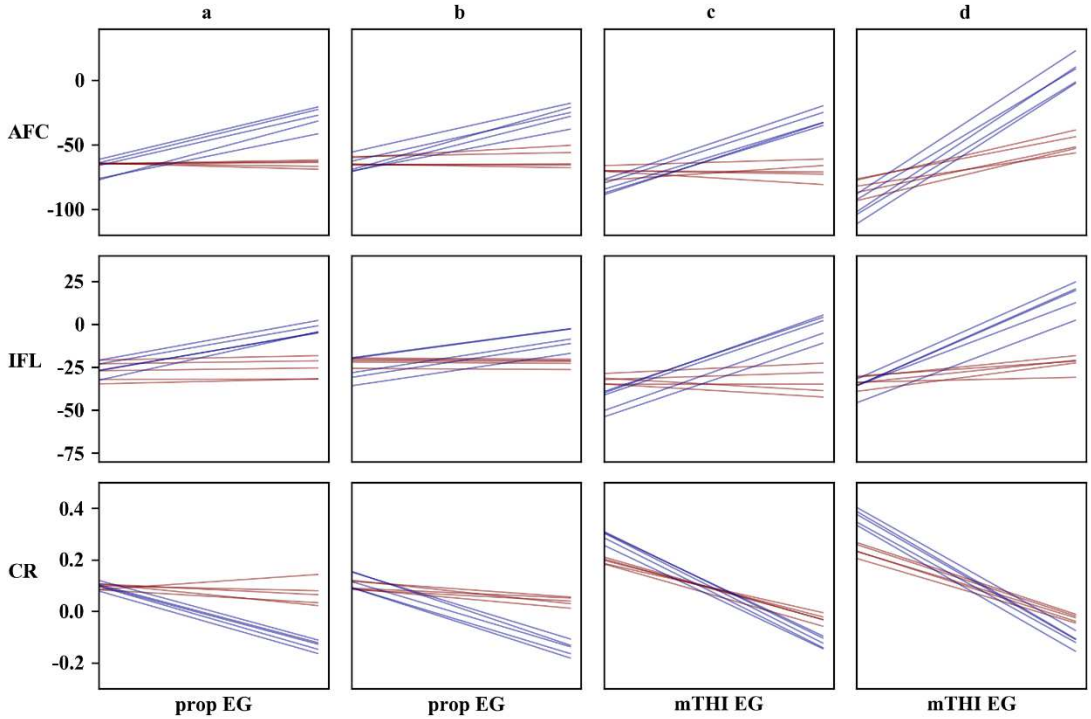

Fig. 4 The re-ranking plots for gEBVs of sires. The blue and red lines represent sensitive and resilient sires, respectively. **a**) Re-ranking plots for three traits estimated using prop-EG under S1. The x-axis is the proportion of days exceeding the threshold with a range of 0 to 1 and y-axis is gEBV. **b**) Re-ranking plots for three traits estimated using prop-EG under S2. The x-axis is the proportion of days exceeding the threshold with a range of 0 to 1 and y-axis is gEBV. **c**) Re-ranking plots for three traits estimated using mTHI-EG under S1. The x-axis is the minimum THI with a range of 15 to 75 and

y-axis is gEBV. **d**) Re-ranking plots for three traits estimated using mTHI-EG under S2. The x-axis is the minimum THI with a range of 15 to 75 and y-axis is gEBV

Single-step genome-wide association analyses

Overall, similar genomic regions were detected to be associated with the same trait when using two scenarios of prop-EG, especially for CR (Figs. 5 and 6). For S1, nine regions were shared for both the intercept and the lope for AFC, among which two (from 26,669,442 to 26,802,092 and from 26,803,676 to 26,880,091 bp) were located in BTA14 and three regions (from 24,762,252 to 25,487,353 bp, from 106,901,044 to 106,946,812 bp, and from 106,948,226 to 106,980,536 bp) in BTA5, respectively. The overlapping region that explained the highest average variance (0.92% for the intercept and 2.30% for the slope) was in BTA14 (from 26,803,676 to 26,927,342 bp). Similarly, the same region (from 26,821,555 to 26,899,089 bp), which is one of the four shared genomic windows, explained 1.12% and 0.91% genetic variance for the intercept and slope of IFL, respectively. For CR, 17 regions were in common between using THI and prop-EG variables in RNM, and a narrower region (from 26,819,709 to 26,888,221 bp) in BTA14, which explained 1.83% and 1.72% genetic variance for the intercept and slope, respectively, was located in the same region detected in AFC and IFL.

The genomic windows explaining the highest variance were not connected for AFC and IFL under S2. However, the area from 26,819,709 to 26,887,021 bp that explained the highest proportion of the total additive genetic variance (2.38% and 2.29% for the intercept and slope, respectively) for CR, was still located in BTA14. We

311 detected 21 overlapping genomic windows for CR between two variables, which is
312 more than detected for AFC and IFL (4 and 13, respectively).

313 More shared genomic regions were detected when the same variables (the
314 intercept or slope) of the two scenarios were tested. For AFC and IFL, more than 10
315 genomic areas were connected in the absence of regions explained the most genetic
316 variance. However, the longest shared region in BTA14 was still detected for both the
317 intercept (from 26,819,709 to 26,887,021 bp) and the slope (from 26,821,555 to
318 26,888,221 bp) for CR. Similarly, more than 25 overlapping areas were mapped for
319 each variable of CR.

320 The Manhattan plots of mTHI-EG are provided in Supp. Files 7 and 8. Basically,
321 more shared regions were mapped when using mTHI-EG compared to prop-EG, but
322 the most associated genomic regions for each trait were found to be distributed in
323 different chromosomes. Detailed information for genomic regions is listed in Supp.
324 Files 9 and 10.

325

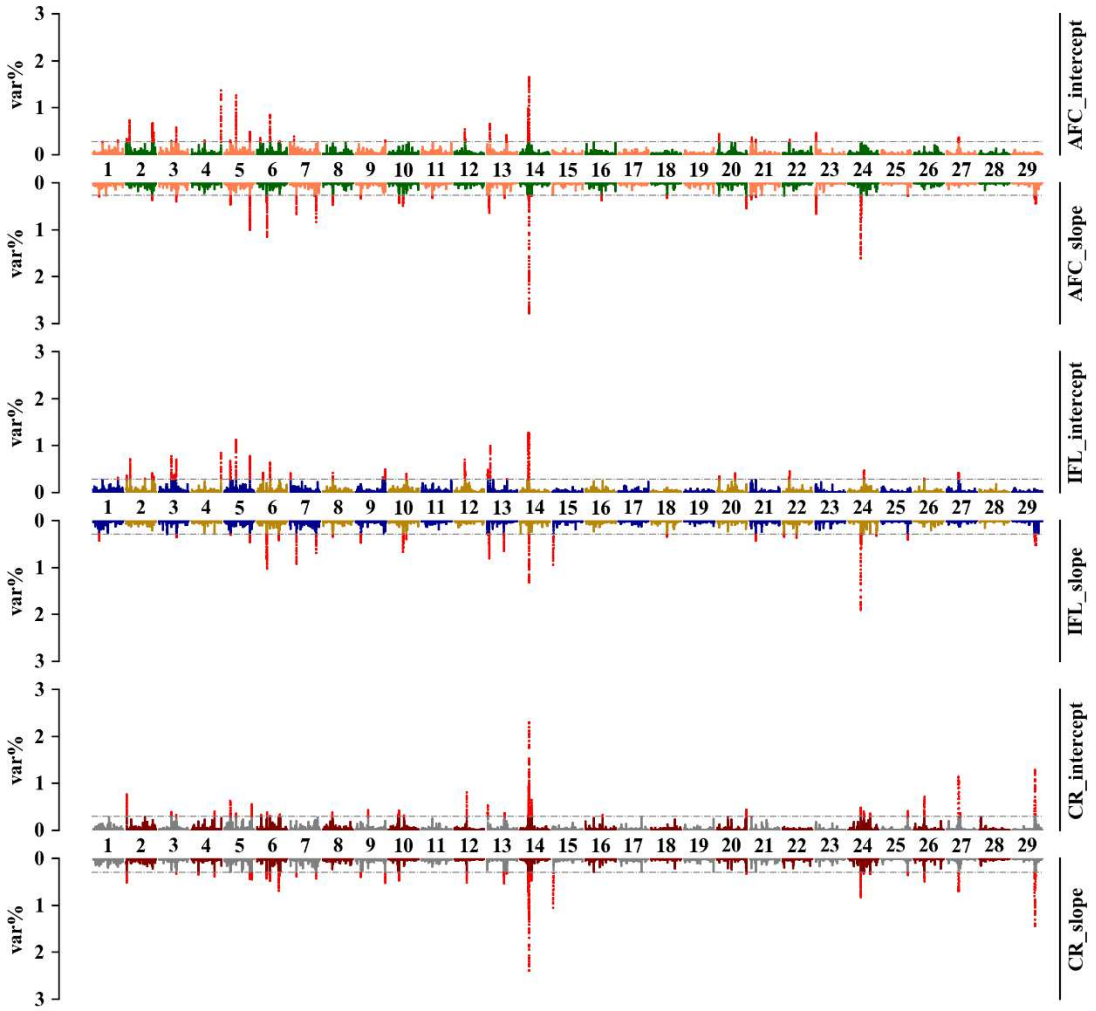

Fig. 5 Percentages of the intercept and slope genetic variances explained by a sliding window of 20 SNPs for three traits, which were estimated under scenario one of prop-EG. The x-axis is autosome segments; the y-axis represents the proportion of explained variances; the grey horizontal lines are thresholds (top 0.5%) for candidate genomic regions; different color sets indicate different traits

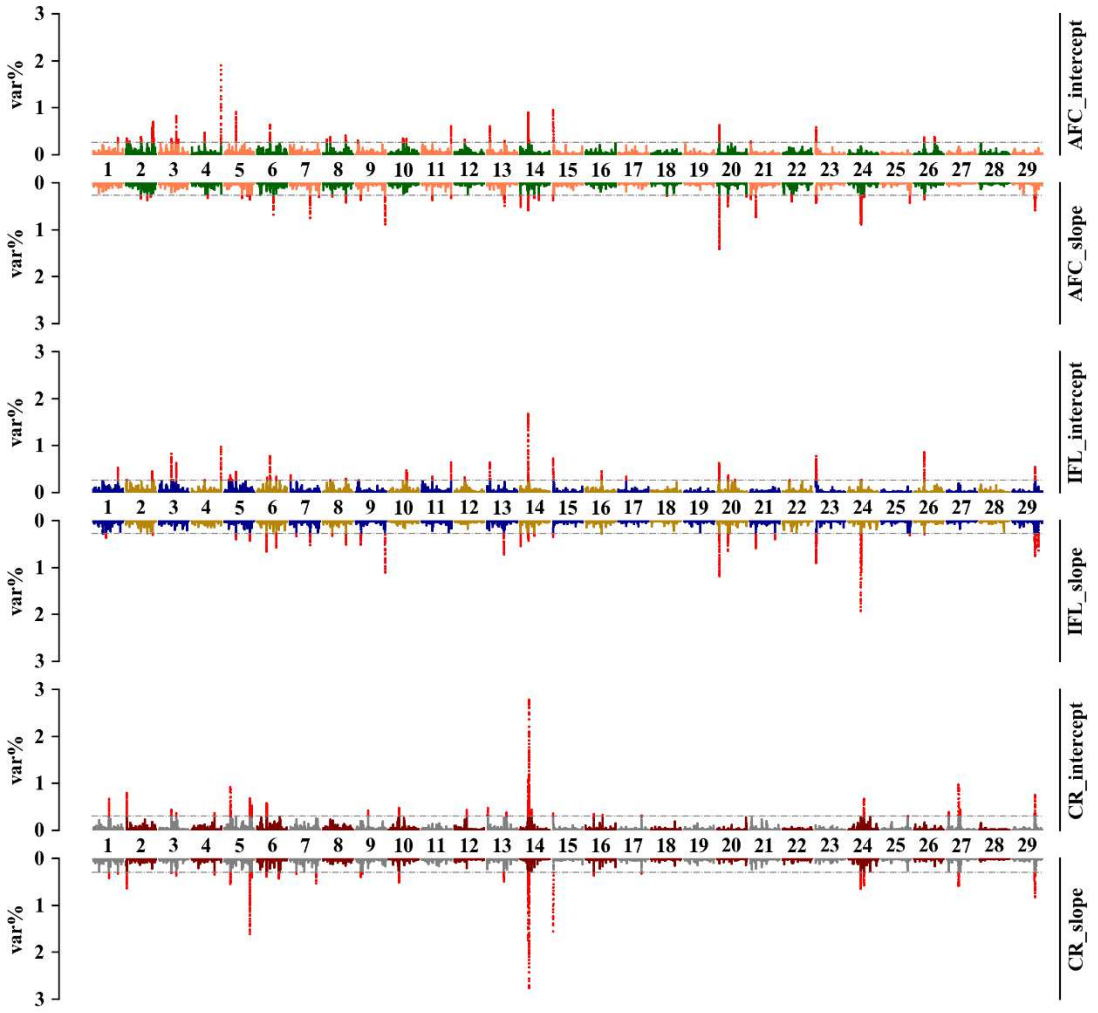

Fig. 6 Percentages of the intercept and slope genetic variances explained by a sliding window of 20 SNPs for three traits, which were estimated under scenario two of prop-EG. The x-axis is autosome segments; the y-axis represents the proportion of explained variances; the grey horizontal lines are thresholds (top 0.5%) for candidate genomic regions; different color sets indicate different traits.

The mapped positional candidate genes are shown in Table 6 and Supp. Files 9 and 10. Candidate genomic regions of the intercept term were previously linked to several types of quantitative trait loci (QTL) such as milk kappa-casein percentage, metabolic body weight, average daily gain, length of productive life, dry-matter intake,

conception rate, and pregnancy rate (Supp. Files 9 and 10). Most of the mapped QTLs are associated with production traits, and the rest are associated with reproduction, health and meat/carcass traits. The identified biological processes ($P < 0.05$) related to heifer reproduction were: developmental process involved in reproduction, oocyte maturation, oocyte development, oocyte differentiation, oogenesis, placenta blood vessel development, and embryo development. Two identified pathways were related to stress response: regulation of response to stress and response to oxidative stress. Other pathways included muscle and body development.

Candidate genomic regions of slope term have been previously linked to a variety of trait groups, including luteal activity, body weight, stillbirth, and many milk-related QTLs. Similarly, most of the QTLs identified were associated with milk production traits, because most of the QTLs overlapped between the two genetic terms. The reproductive biological processes identified ($P < 0.05$) using the slope term were: reproductive processes, fertilization, sexual reproduction, granulosa cell differentiation, oocyte development, acrosome reaction, oocyte differentiation, and regulation of luteinizing hormone secretion (Supp. Files 9 and 10). Additionally, more potential stress-related pathways were identified such as response to abiotic stimulus, detection of stimulus involved in sensory perception, response to temperature stimulus, response to radiation, negative regulation of saliva secretion, aerobic respiration, and energy derivation by oxidation of organic compounds.

Table 6 Genes and QTLs for top genomic regions of two environmental gradients.

EG[a]	Trait[b]	Covariable	Chromosome	Genes	Var%	#QTL	QTL traits
Prop-EG	AFC	slope	BTA14	*CLVS1*	2.30	1	Milk unglycosylated kappa-casein percentage
	CR	intercept	BTA14	*CLVS1*	2.29	3	Milk kappa-casein percentage
	CR	slope	BTA14	*CLVS1*	1.83	1	Milk kappa-casein percentage
	CR	intercept	BTA14	*CLVS1*	1.72	2	Milk kappa-casein percentage
	AFC	slope	BTA14	*LOC112449637*	1.49	1	Milk unglycosylated kappa-casein percentage
	CR	slope	BTA5	*FKBP4, DDX11*	1.20	3	Bovine tuberculosis susceptibility, Milk kappa-casein percentage
mTHI-EG	AFC	intercept	BTA14	*CLVS1*	2.27	1	Milk glycosylated kappa-casein percentage
	AFC	slope	BTA14	*CLVS1*	2.03	1	Milk unglycosylated kappa-casein percentage
	AFC	slope	BTA14	*LOC112449637*	1.80	1	Milk unglycosylated kappa-casein percentage
	CR	intercept	BTA14	*CLVS1*	1.39	3	Milk kappa-casein percentage
	CR	slope	BTA5	*FKBP4, DDX11*	1.35	2	Milk kappa-casein percentage

	CR	slope	BTA14	*CLVS1*	1.34	3	Milk kappa-casein percentage

[a] prop-EG = the number of days that exceeding the threshold temperature humidity index in the period; mTHI-EG = minimum temperature humidity index for each day of the period

[b] AFC = age at first calving; IFL = interval from the first to last service; CR = conception rate of first service

Cluster analysis for SNP effect trajectories

The pattern of SNP effects over different EGs of each trait, scenario, and cluster are shown in Fig. 7. The SNP effects remained at a specific level within each trait, and the effects of CR were almost 100 times less than those of AFC and IFL. The magnitude of SNP effects changes was higher for S2 (red lines) in all traits and EGs in C1 and C2, whereas the SNP effects in C3 were similar in each trait and scenario. The cross point of different clusters appeared later when mTHI-EG was used. Furthermore, lower standard deviations were observed for CR in different scenarios and clusters.

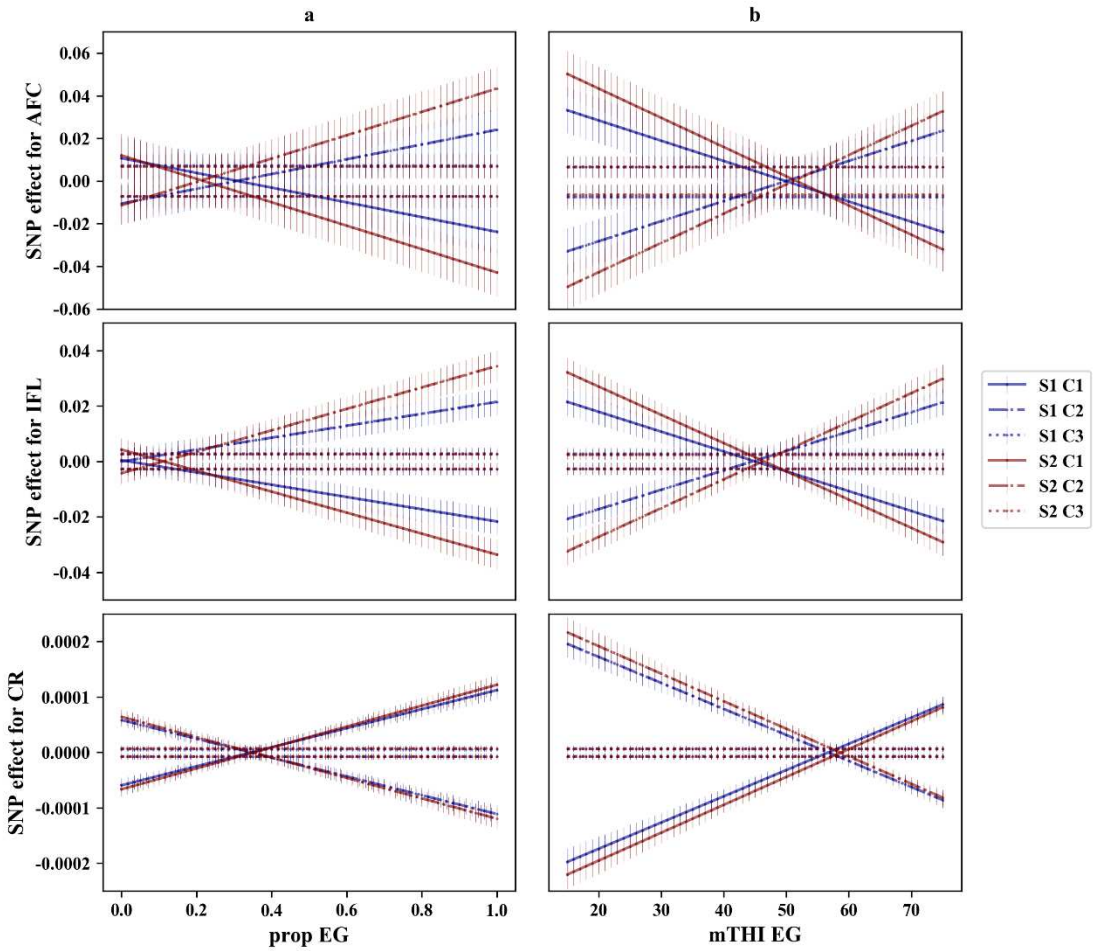

Fig. 7 Trajectories of SNP effects changing over EGs. The x-axis is environmental gradient; the y-axis represents the SNP effects; vertical bar is the standard deviations of SNP effects at each level of EG; blue lines indicate scenario one; red lines indicate scenario two; different color sets indicate different clusters. **a**) Trajectories of SNP effects changing over prop-EG. The x-axis is the proportion of days exceeding the threshold with a range of 0 to 1. **b**) Trajectories of SNP effects changing over mTHI-EG. The x-axis is the minimum THI with a range of 15 to 75.

Approximately 50 overlapped genes were identified in C1 and C2, whereas 10 or 17 shared genes were detected in C3. However, over 330 positional genes were

391 detected within each trait in C3, which is nearly twice the number of genes mapped in
392 C1 and C2 (Fig. 8). Additionally, the number of overlapping genes between AFC and
393 IFL was found to be higher than those shared with CR in C1 and C2. A total of 149
394 common genes were identified in different clusters, among which 50 genes overlapped
395 between prop-EG and mTHI-EG.
396

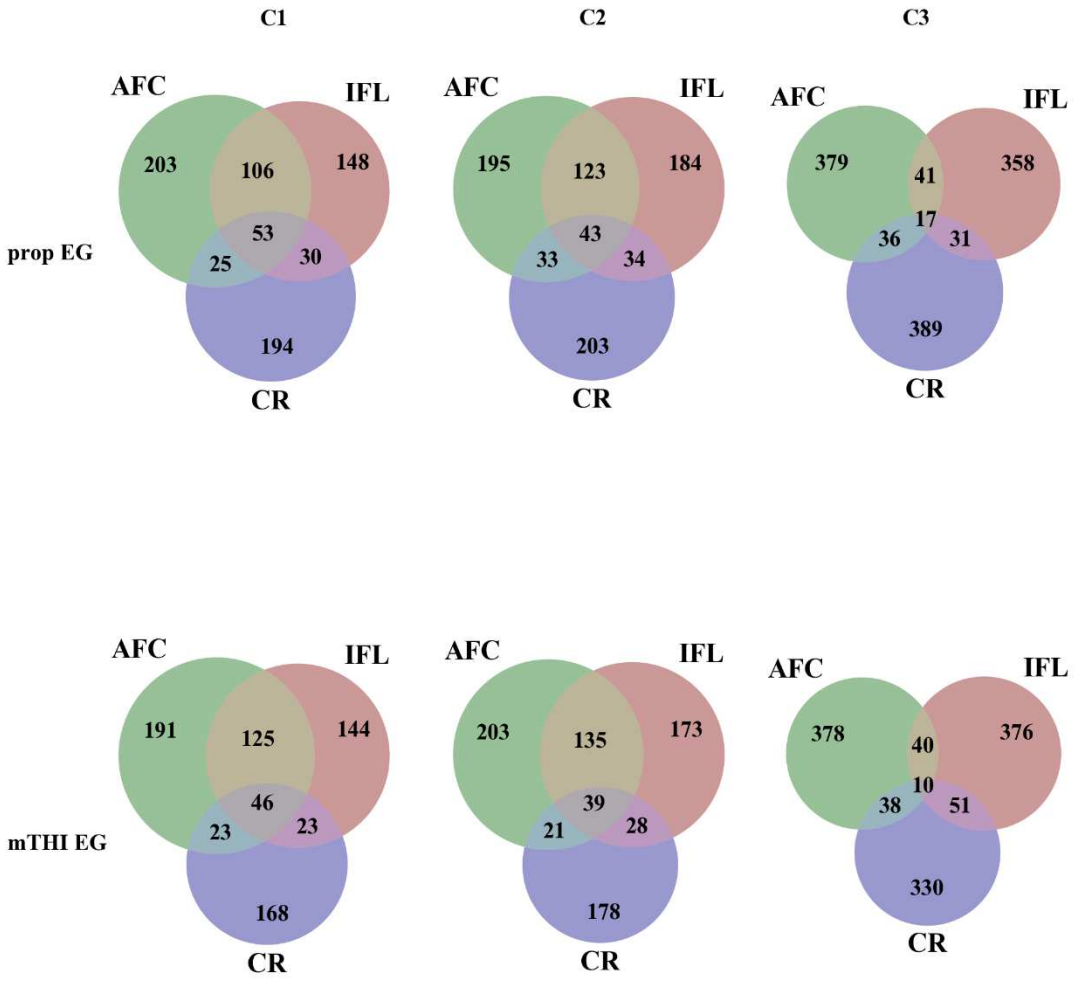

397

398 **Fig. 8** Number of shared candidate genes for each EG in different traits and clusters.
399 C1 = SNP effects changes in preferential ways (decrease for AFC and IFL; increase for
400 CR); C2 = SNP effects changes in the opposite ways (increase for AFC and IFL;
401 decrease for CR); C3 = constant SNP effects over time.

DISCUSSION

Heritabilities estimated from the conventional animal model

The heritability estimates were 0.03 (0.005) for CR, 0.06 (0.007) for IFL and 0.16 (0.011) for AFC (Table 1). The heritability of AFC in our study was at a similar level as that estimated previously (0.07–0.24) [23]. For heifer IFL and CR, the heritabilities observed agree with earlier studies in Irish Holstein population [23] and in the same Chinese Holstein populations [4]. The current study showed that heritability estimates for interval traits (AFC and IFL) were generally higher than for the binary trait (CR), which is also consistent with several studies [7, 24, 25].

The influence of heat stress on heifer fertility traits

Several studies have demonstrated that heat stress may have adverse effects on heifer fertility in two aspects [26]: (1) follicular development or estrus, and (2) pregnancy. The percentage of Holstein heifers having two follicular waves in the heat-stressed group (33 °C, 60% relative humidity) and thermoneutral group (21 °C, 60% relative humidity) have been shown to be 18% and 91%, respectively; the day of functional luteolysis was delayed for almost 9 days in the heat-stressed group, compared with the controlled group [27]. Sakatani et al. [28] found that the estrus detection rate of non-lactating Japanese Black cows was significantly lower in summer, whereas another study of lactating Holsteins also illustrated that the estrus detection rate decreased when THI exceeded 72 [14]. Follicular development and estrus detection

424 are negatively affected by heat stress, which extends AFC and IFL. Another analysis of
425 20,606 cows also showed that pregnancy rates declined when THI was greater than 72,
426 with a decrease in pregnancy rate of 1.03% per unit increase of THI [29]. In the current
427 study, a dramatic decrease in the month of July was observed for the CR phenotypes
428 (Suppl. File 11), which is consistent with the results of previous studies.

429 The critical periods found under S2 of CR, on the basis of first insemination day,
430 were (-10, 60) and (-10, 30) for prop-EG and mTHI-EG, respectively, which are similar
431 to the values reported in previous studies. Khan et al. [17] explored the effects of heat
432 stress on the pregnancy rate using 1,100 crossbred dairy cows in India and reported that
433 pregnancy rates decreased significantly when cows experienced high THI (>72) within
434 a period of at least 30 days before and after the insemination day. For AFC and IFL,
435 the critical period was earlier before the first service: (-90, -30) or (-90, -60). This may
436 be partly due to the delay of first insemination; that is, follicular development or estrus
437 detection may be compromised by heat stress. A study evaluating the whole cycle of
438 estrus showed that heat stress inhibits the development of the dominant follicle during
439 preovulatory period in heifers [27]. Thus, the onset of estrus for heifers would be
440 delayed to the next circle due to the delayed development of follicles, and heat stress
441 actually impacts the heifers earlier before the first insemination. Another possible
442 explanation is that heat stress may affect puberty of heifers. The age at puberty is
443 generally 13 months, and the average age at first service in this study was 491.95 days
444 (around 16 months) with a standard error of 72.48 days. This may explain the reason
445 that the boundary of the critical periods for AFC and IFL was found to be 90 days (3

446 months) before the first insemination. However, additional studies are needed to
447 validate this relationship.

448 To the best of our knowledge, the critical periods of heat stress for heifer
449 reproduction traits have not been well defined, and most studies focused solely on
450 pregnancy rate or CR. Amundson et al. [30] detected negative associations of THI with
451 pregnancy rate for *Bos taurus* crossbred cows in all three breeding periods: (0, 21), (0,
452 42) and (0, 60). Another study indicated that a high heat load 3-5 weeks before and 1
453 week after service was associated with reduced CR in cattle [31]. In [18], the CR of
454 lactating dairy cows was negatively affected by heat stress both before and after the day
455 of insemination (-42, 31), with the greatest negative impact in (-21, -1). The results of
456 the current research indicated that the critical period of heat stress is trait-related, and
457 the periods we identified for CR are within the range reported in previous studies, which
458 provides substantial support for the results of AFC and IFL.

459 The overlapping test of the two EGs under two scenarios (Table 3) indicated
460 that prop-EG and mTHI-EG capture different mechanisms. For instance, prop-EG
461 equaled 0.5 in a period of 60 days when the THI of any 30 days in this period exceeded
462 the threshold. However, the average daily THI of these 30 days may be 73 or 78 (more
463 severe heat stress). Similarly, prop-EG equaled 0 when THI did not exceed the
464 threshold for all the days in a period, but these days may occur in autumn or winter
465 (cold stress). Consequently, prop-EG could not assess cold or severe heat conditions as
466 mTHI-EG; it represents the average heat load of heifers, i.e., the proportion of days
467 experiencing heat stress conditions, which would not include all the climatic variation

468 due to the use of a THI threshold. Compared with AFC and IFL, CR may be more
469 sensitive to climatic changes, as it produced fewer overlapping animals between the
470 two EGs.
471
472 **Variance components estimated from RNMs and G × E**
473 We estimated variance components using RNMs with the matrices ***A*** and ***H***
474 (Table 4 and Supp. File 4). The genetic variances obtained from conventional RNMs
475 and those from genomic RNMs were similar for all traits and agree with the results of
476 previous studies (e.g., [7, 32]). Heritabilities estimated from RNMs were generally at
477 similar levels, compared with those estimated from conventional animal models (Fig.
478 2). Zhang et al. [7] detected heterogeneities in heritabilities across different EGs for
479 fertility traits from both matrices, which is consistent with our study. A recent study
480 found the genetic variances of production traits varied in different THI levels, and a
481 quadratic curve was observed in the heritabilities of protein yield [8]. In Danish
482 Holstein populations, heterogeneities of heritabilities of several fertility traits were
483 observed across different production levels or grass ratio in feed [6, 33]. Although
484 heritabilities vary across EGs in different analyses, patterns of heritabilities with
485 changes in the environment are predictable. Various environmental indicators and
486 analyzed traits could account for this result. Heterogeneities in heritabilities provide the
487 insight that future genetic evaluations should consider different environmental
488 variances to obtain accurate results. Incorporating heat stress into breeding objectives

could be helpful for the correct selection of animals in different environments, especially in countries where climatic conditions are highly variable.

Based on the t-test for the variance of the slope, a statistically significant G×E was observed for all traits in this study [5]. Moderate to strong negative correlations were detected between the intercept and slope for each trait. This negative relationship was also found by other researchers who estimated the variance components of cow fertility traits using RNM [6, 7]. Previous studies have suggested that a low correlation between the intercept and slope could indicate re-ranking of animals across different environments [34, 35]. In addition, Liu et al. [6] illustrated that this negative correlation could increase the magnitude of G×E. Collectively, robust animals with preferential intercepts and flat slopes are able to perform well across various environments [36]. Based on RNMs, individual breeding values for each THI condition can be appropriately estimated to enable selection of heat tolerant cows. These estimates could be more accurate for bulls whose daughters have different records under different environments. Genetic correlations between different EGs estimated using conventional and genomic RNMs were almost the same (Fig 3 and Supp. File 5). The larger the difference between the two EGs, the less they were correlated, which is consistent with studies using different EGs [6, 7, 37]. This indicates that the re-ranking of sires may occur in different EGs, as indicated in Table 5. The re-ranking was more obvious for CR, compared with the other two traits, indicating that CR has a higher sensitivity under different THI. As mentioned in the previous section, heat stress has adverse effects on follicular development, which is directly associated with conception.

Furthermore, we observed that the re-ranking was stronger when using mTHI-EG for AFC and IFL, which validates the hypothesis that mTHI-EG captured more variation in environments than prop-EG.

In a breeding scheme for improved heat tolerance, the best approach could involve selecting the best-performing individuals in heat stress conditions, provided that they are not underperforming in thermoneutral conditions. These robust animals can be presented graphically as shown in Fig. 4. For these traits, all animals have consistent intercepts, whereas the gEBVs of heat-tolerant heifers (red lines) did not change dramatically along all environmental conditions. The less the AFC and IFL, the greater the farm profit. All the robust heifers performed better in higher THI conditions. Adverse trends were observed for CR because a higher CR is preferential. The magnitude of re-ranking was higher when using mTHI-EG. This is additional evidence that mTHI-EG is more sensitive than prop-EG.

Candidate genomic regions for the intercepts and slopes

We performed ssGWAS to detect candidate genomic regions associated with heifer fertility and heat sensitivity (Figs 5 and 6, Supp. Files 7 and 8). Some identified genomic regions are common between two traits or two variables in the same trait (Supp. Files 9 and 10). Generally, most of these genomic regions explained a small (< 1%) proportion of the total additive genetic variance, indicating that fertility and heat tolerance are largely polygenic traits. However, the functional analysis confirmed that the fertility traits are influenced by heat stress. For example, some of the genomic

regions were previously reported to be associated with pathways such as response to abiotic stimulus, detection of stimulus involved in sensory perception, response to temperature stimulus, response to radiation, negative regulation of saliva secretion, and aerobic respiration and energy.

As expected, the genomic regions associated with the intercept (average performance in thermoneutral conditions) were linked with several reproductive genes. For example, the overlaps of genomic windows between the intercept of AFC and IFL contained genes such as *AMHR2*, *SP1*, *KRT8*, and *KRT18*. Ilha et al. [38] found that the mRNA expression levels of *AMHR2* decreased in the follicles during follicular deviation, whereas another study also indicated that *AMHR2* plays a role in follicular development by regulating granulosa cells [39]. *KRT18* may be a molecular marker for bovine microfold cells in the follicle-associated epithelium [40]. Together with *KRT8*, these two keratin family genes influence the bovine estrous cycle with regards to luteal cells [41]. *SP1* has been demonstrated to co-express with other regulators to control early placental differentiation [42]. *PLAG1*, which was mapped in the most evident region of BTA14 for AFC and IFL, has been often reported to be associated with growth and reproduction traits in cattle [43–45]. The overlapping genomic regions between AFC and CR contained other growth-related genes, such as *SDC3* [46] and *FABP3* [47]. One possible explanation is that most heifers are physiologically immature at the time of first insemination.

Various candidate genes associated with heat tolerance (slope term) were also reported in the literature. Several candidate genes are related to cow reproduction, for

example, *GPER1*, which has been reported to induce the non-genomic suppression luteinizing hormone secretion in cattle [48], was mapped in both AFC and IFL in the genomic region of BTA25. *RAD51* has been reported to be associated with bovine oocytes meiosis progress [49, 50]. Some candidate genes (e.g., *LAP3*, *GLYCAM1*, *PDE1B*, *MICALL2*, *NPC1*) are related with other economic traits in cattle such as milk production, carcass traits, body weight, body height, and body length [51–55]. Additionally, several genes were annotated to be associated with stress response in cattle. *HCRTR1*, which regulates orexin receptor type 1, has been suggested to participate in negative feedback regulation in the adrenal gland [56]. Several studies examined cultured bovine adrenal cells and indicated that the products of *AGRP* would inhibit the cortisol production of adrenal gland [57, 58]. The stress reaction of animals activates the hypothalamic-pituitary-adrenal axis, together with an increase in the cortisol concentration [59]. Thus, *HCRTR1* and *AGRP* may play vital roles in the cattle stress reaction process. White et al. [60] reported that endogenous *PC* expression in bovine primary hepatocytes and kidney epithelial was significantly higher in thermal stress conditions, which indicated that *PC* may contribute to the physiological response to thermal stress. *PC* has been reported to be associated with fatty acids regulations while feeding and thus affect the feed intake of cattle [60, 61].

The biological processes identified in functional analyses were mainly reproduction- and stress response-related, which corroborates our findings. The QTLs we found were mainly milk and production associated (Supp. Files 9 and 10), indicating that these economic traits may change as the climate conditions become more extreme.

577 Most of the QTLs overlapped when using different EGs, and many were located in
578 BTA14. Costa et al. [62] reported that the QTLs in BTA14 (24.3 Mb) and BTA24 (23.4
579 Mb) are associated with AFC in Nellore. The genomic regions detected from 23 to 26
580 Mb in BTA14 and BTA24 were most evident in the Manhattan plots among the
581 different traits and EGs. Mota et al. [45] supported that the region of BTA14 plays a
582 key role in the puberty of heifers through growth hormone signaling and may be
583 regulated by *PLAG1*. Another genomic region with high genetic variance is located in
584 BTA29 (from 44.3 to 44.9 Mb), which includes the heat stress-related gene *PC*. Most
585 of the QTLs were shared by the intercept and slope, which is consistent with the strong
586 negative genetic correlations between them. The fertility-related QTLs would be
587 evident in heat stress conditions as well because the change in environments may alter
588 the genetic expression of these regions when a strong G×E exists.
589
590 **Clustered SNP effects and genes**
591 The trajectory of SNP effects over EGs (Fig. 7) suggests a substantial SNP by
592 environment interactions, which has also been reported for reproduction traits in pigs
593 [32] and cattle [45]. The dramatic changes in C1 and C2 in S2 indicates that the critical
594 periods, which were chosen through AIC, may capture more genetic variation. As for
595 CR, half of the periods overlapped in S1 (-30, 30) and S2 (-10, 30 or 60), which may
596 explain the similarity in the trajectories between the two scenarios. For C1 and C2, the
597 variation in SNP effects was greater at high levels of prop-EG (Fig. 7a) than at low or
598 middle levels, which was expected due to the higher genetic variance detected at high

599 prop-EG levels compared to low and middle prop-EG levels (Fig. 2a). Similarly, this
600 explains the greater SNP effects at both high and low levels of mTHI-EG and the late
601 “cross point”, which represents the lowest genetic variance at middle mTHI-EG levels
602 (Fig. 2b). These findings agree with those of Silva et al. [32]. The effects of top SNPs
603 were more constant (lower standard deviation) in CR compared with AFC and IFL.
604 This finding may be due to the relatively low heritability of CR, which causes smaller
605 effect variations in each level of EG.

606 Three SNP clusters were inspected to identify common genes among all the
607 fertility traits (Fig. 8). As expected, more candidate genes were shared between interval
608 traits (AFC and IFL), especially in C1 and C2. The number of overlapping genes among
609 all the traits and EGs were comparable for each cluster. For C3, the top SNPs with slope
610 effects close to 0 were chosen, but the variation was negligible, i.e. SNP effects of the
611 slope ranged from 9.48e-9 to 1.47E-11 for all traits. Thus, a slight change in the effect
612 estimates may cause re-ranking of SNPs, which results in a small proportion of shared
613 genes among traits in C3. The trajectories of C1 and C2 (Fig. 7) indicate the existence
614 of SNP by environment interactions, which indicate that some related genes may be
615 activated at specific temperature and humidity levels. Thus, candidate genes that play
616 an important role in SNP effect changes (C1 and C2) are the priority of the current
617 research.

618 Some genes detected in both EGs were reproduction– or milk–related. For
619 instance, *MLH1* is associated with oocyte development [50] and *EOMES* plays a vital
620 role in the early pregnancy stage of ruminants. Sakurai et al. [63] reported that cattle

EOMES expression increases when conceptuses attach to the uterine epithelium. In a Chinese Holstein population, Han et al. [64] profiled the genetic effect of *ACACB*, which affects milk composition traits, using whole genome re-sequenced data. As production and reproduction traits are genetically related [2], it is reasonable that some production associated genes were also detected in this study.

When prop-EG was considered, reproductive genes *NR5A2*, *THBS2* and *PRKCE* were identified. *NR5A2* was mapped in C1, and it has been reported to affected steroidogenic pathways of progesterone production during the luteal phase of the estrous cycle in cattle [65]. *THBS2* and *PRKCE* contain several candidate SNPs in C2, and their potential luteolytic functions were illustrated in previous studies [66, 67]. Additionally, *EGFR*, whose expression is related with bovine reproduction stage [68], was detected in both C1 and C2. Wijayagunawardane et al. [69] explored the potential mechanisms responsible for the detrimental effect of heat stress by exposing bovine oviductal epithelial cells to heat stress conditions (40 and 43℃). The results indicated that *EGFR* could be involved in the regulation of the bovine oviductal microenvironment, but these regulatory mechanisms may be compromised in the presence of heat stress. This indicates that the regulatory functions of detected reproductive (or even milk- and growth-related) genes might be compromised in heat stress conditions. Thus, these altered SNP effects were observed at higher levels of prop- and mTHI-EGs (Fig. 7).

When mTHI-EG was used, *GUCY1B1* was identified in C2. Several papers [70, 71] have demonstrated that *GUCY1B1* interacts with heat shock protein 90 (*HSP90*),

whereas Khan et al. [72] detected *HSPA13* as a differentially expressed gene in heat-stressed bovine granulosa cells. This indicates that the interaction between *GUCY1B* and *HSP90* in cattle may be related to the heat stress response.

CONCLUSIONS

In the present study, we analyzed the impacts of heat stress on dairy cattle based on three reproductive traits. The critical periods, which are when heifers may be easily affected by heat stress, were found to be related to the environmental gradient used, centered on the first insemination day. This indicates that detailed analysis for other traits should be applied to derive this period. Genetic parameters suggest significant and considerable magnitude of G×E for all three heifer fertility traits, indicating that breeding values may change under heat stress conditions for these traits. The re-ranking of sires between different environments further demonstrates the effects of G×E on animal breeding. Several reproduction–, growth–, production–, and resilience–related genes and QTLs were identified in the candidate genomic regions affecting fertility traits. Overall, G×E models should be integrated into current dairy cattle breeding schemes to select more climatic resilient animals. The heat stress-related genes or QTLs are important for exploring the mechanisms of heat stress response in dairy cattle.

MATERIALS AND METHODS

Data

664 Field records of birth, service and calving during 2005 – 2018 for heifers raised
665 in 15 Holstein farms (Sunlon Livestock Development Co. Ltd) in Beijing, China, were
666 collected from the herd management software AfiFarm (AfiFarm,
667 www.afimilk.com.cn). All herds were kept in a free-stall design and included 1,000 to
668 2,000 heifers and the management strategies of these farms are assumed similar. The
669 analyzed heifer traits are AFC (age at first calving), IFL (interval from the first to last
670 service), and CR (conception rate of first service). CR was coded as 1 when there was
671 a confirmed pregnancy after the first service and 0 otherwise. The number of interval
672 days is 0 when a heifer is pregnant after the first service. Further criteria for the data
673 editing included AFC between 500 and 1,100 days and IFL between 0 and 365 days.
674 Records exceeding these thresholds were dropped. Animals which changed herds
675 during the analyzed period were excluded. The number of records for each trait after
676 editing are 56,998 (Table 1). The pedigree was derived from field birth records and
677 each animal was traced back at least three generations. The final pedigree contains
678 181,693 individuals, among which 6,556 are sires.
679 Phenotypes (of daughters) and genotypes were available for 3,731 heifers and
680 537 bulls. All bulls and a subset of 2,379 heifers were genotyped using the GeneSeek
681 Genomic Profiler Bovine 50K Chip, whereas the remaining 1,352 heifers were
682 genotyped using the GeneSeek Genomic Profiler Bovine 150K Chip. In addition, 1,769
683 heifers genotyped with the 150K chip were included in the reference population to
684 improve imputation accuracy. The animals genotyped with the 50K chip were imputed
685 to the 150K using the Beagle v5.0 software [73] with an expected imputation accuracy

686 greater than 0.95. After imputation, SNP markers were filtered by removing markers
687 with minor allele frequency lower than 0.05, missing rate greater than 0.10 and
688 presenting extreme deviation from the Hardy–Weinberg equilibrium (P ⩽ 10E−5).
689 Individuals with genotype call rate lower than 0.90 were dropped and only autosomal
690 markers were retained for this study. After quality control, 111,068 SNPs remained in
691 the dataset.

692 Hourly recorded temperature data of Beijing (all farms are within 30 km from
693 the weather station) during the test years were obtained from the National Oceanic and
694 Atmospheric Administration (www.noaa.gov). Hourly THI was calculated using the
695 following formula [74]:

696 $$THI = T_{db} + (0.36T_{dp}) + 41.2$$

697 where T_{db} is the hourly dry bulb temperature (°C) and T_{dp} is the dew point temperature
698 (°C). Then, the daily THI was calculated by averaging hourly values.

699

700 **Models**

701 Variance components were obtained using the following single-trait animal
702 model:

703 $$\mathbf{y} = \mathbf{Xb} + \mathbf{Za} + \mathbf{e}$$

704 where **y** is the phenotype of each heifer for the three fertility traits (AFC, IFL, and CR);
705 **X** is an incidence matrix connecting the vector of fixed effects **b** (herd-year-month of
706 the first service, service technician and sexual-controlled semen) to **y**; **Z** is an incidence

matrix connecting **a** (additive genetic effect) to **y**, and **e** is the residual effect. The following RNM was used to investigate G×E:

$$\mathbf{y} = \mathbf{Xb} + \mathbf{Z_0a_0} + \mathbf{Z_1a_1} + \mathbf{e}$$

where $\mathbf{Z_0}$ is an incidence matrix connecting $\mathbf{a_0}$ (intercept) to **y**, and $\mathbf{Z_1}$ is an incidence matrix containing EGs as covariables to connect $\mathbf{a_1}$ to **y** (slope). It was assumed that $\begin{bmatrix} \boldsymbol{a}_0 \\ \boldsymbol{a}_1 \end{bmatrix} \sim \boldsymbol{N}\left(0, \boldsymbol{K} \otimes \begin{bmatrix} \sigma^2_{a_0} & \sigma_{a_0a_1} \\ \sigma_{a_0a_1} & \sigma^2_{a_1} \end{bmatrix}\right)$, where $\boldsymbol{K}$ is $\boldsymbol{A}$ (numerator relationship matrix) for pedigree-based BLUP models, or to $\boldsymbol{H}$ (combined pedigree-genomic relationship matrix) for ssGBLUP models.

The matrix $\boldsymbol{A}$ was constructed using pedigree data only for conventional BLUP models, whereas for the ssGBLUP models, the inverse of the $\boldsymbol{H}$ matrix ($\boldsymbol{H^{-1}}$), which was calculated as follows [20, 75]:

$$\boldsymbol{H^{-1}} = \boldsymbol{A^{-1}} + \begin{bmatrix} 0 & 0 \\ 0 & \boldsymbol{G^{-1}} - \boldsymbol{A_{22}} \end{bmatrix}$$

where $\boldsymbol{A_{22}}$ is the subset of **A** for genotyped individuals and $\boldsymbol{G}$ is the blended genomic relationship matrix. $\boldsymbol{G}$ was built using $(1 - \omega)\boldsymbol{G_0} + \omega\boldsymbol{A_{22}}$, where ω is the assumed weight of the genetic variance not captured by markers and was set to 0.05 according in previous studies [7, 76]. $\boldsymbol{G_0}$ was constructed using the method proposed by [77]. Finally, $\boldsymbol{G}$ was tuned to have the same scale as $\boldsymbol{A_{22}}$ [78, 79].

The random residual vector **e** is assumed to follow $\mathbf{N} \sim (0, \mathbf{I}\sigma^2_{\mathbf{e}})$, where **I** is an identity matrix. The residual variances were assumed to be the same across different EGs, based on the results of preliminary analyses, which suggested that residual variances were similar across different levels of EG. The full data was divided into

three subsets based on the percentile of EGs (percentiles of EG of ≤0.1, 0.1–0.3, and ≥0.3) to achieve similar sample sizes across subsets.

The (co)variance components for RNMs were estimated using the average information REML method implemented in the BLUPF90 programs [80]. The standard errors of (co)variance components were obtained from the average information matrix. The standard errors of heritabilities among different EGs were calculated using the Taylor series expansions [81].

Critical period and environmental gradient

To evaluate the impact of heat stress on heifer reproduction, the basic assumption was that heifers experiencing higher THI in a specific period have reduced fertility performance based on critical periods, as defined in Fig 1. The levels of prop-EG range from 0 to 1 according to its definition. For mTHI-EG, the levels of EG are the true minimum THI value, ranging from 15 to 75. Two scenarios were included in each EG to select critical period: 1) Scenario 1 (S1) contained only one reference period of 60 days, which goes from 30 days prior to the first insemination to 30 days after the first insemination [17] for three reproductive traits and two EG schemes; scenario 2 (S2): the critical periods were selected based on the AIC of RNMs, which resulted in different critical periods for each trait or EG scheme. A total of 19 combinations were tested in S2, and periods with the lowest AIC were chosen (Supp. File 2). For each trait, two critical periods (S1 and S2) were chosen under each EG (prop-EG and mTHI-EG) to estimate the (co)variance components of the RNMs. The relationships of the two EG

schemes were also evaluated by calculating the equivalent values: the proportion of days exceeding threshold THI when the average minimum THI of this period at a certain level. Afterwards, the overlapping heifers were counted for each equivalent environmental condition between two EG schemes.

Magnitude of G×E

G×E exists if the variance of the slope was significantly different from zero by using a one-tailed t-test with the significance level of 0.05 [6, 33]. One possible consequence of G×E is the re-ranking of animals across different environments [5]; thus, the top 50 sires with at least 20 daughters having phenotypes were selected to assess the magnitude of re-ranking. Re-ranking plots were drawn to show the change pattern of breeding values for sires with the most preferential intercepts or with the lowest slopes.

Single-step genome-wide association study (ssGWAS)

The marker effects of the intercept and the slope for all traits were estimated using the ssGWAS method proposed by Wang et al. [21]. The percentage of genetic variance explained by a moving genomic window of 20 adjacent SNPs was obtained, by applying the postGSf90 package [82]. The number of adjacent SNPs were defined based on the level of linkage disequilibrium in this population, following [7]. The top 0.5% genomic regions that explained the highest genetic variance of intercept or slope was considered as the candidate genomic regions. Subsequently, candidate genes or

QTLs within the candidate genomic regions were annotated based on the ARS-UCD1.2 genome (http://hgdownload.soe.ucsc.edu/goldenPath/bosTau9/bigZips/genes/) and the Cattle QTL database (https://www.animalgenome.org/cgi-bin/QTLdb/). The biological processes of candidate genes were annotated using the PANTHER Classification System [83].

Cluster analyses of relevant SNPs

The SNPs were chosen to investigate the trajectories of their effects. Firstly, SNPs were ranked according to the magnitude of their slope effects for each trait, EG, and scenario. Then, three clusters (C) of SNPs were obtained according to the trajectory of their SNP effects across each EG: C1 = SNP effects changes in preferential ways (decrease for AFC and IFL; increase for CR); C2 = SNP effects changes in opposite ways (increase for AFC and IFL; decrease for CR); C3 = constant SNP effects over time. For C1 and C2, the top 0.5% (n=555) SNPs with the highest or the lowest slope effects were selected, whereas for C3, the 0.5% SNPs with slope effects closest to zero were selected. Choosing the top 1% SNPs for trajectory analyses has been implemented in several GWAS studies based on the 50K SNP panel [32, 84]. The results were visualized based on the average and standard deviation of SNP effects in each EG to show the differences among the three clusters. For C3, SNPs were grouped into two categories according to their average effects (lower or higher than 0). Only the genes containing SNPs further confirmed in the cluster analysis and shared among three traits were further annotated for biological functions.

ABBREVIATIONS

G × E: Genotype by environment interaction; QTL: Quantitative trait loci; THI: Temperature humidity index; EG: Environmental gradient; RNM: Reaction norm model; BLUP: Best linear unbiased predictor; ssGBLUP: Single-step genomic BLUP; ssGWAS: Single-step genome-wide association study; AFC: Age at first calving; IFL: Interval from first to last service; CR: Conception rate; prop: The proportion of days that exceeded the threshold THI in candidate period; mTHI: minimum THI for each day of the candidate period; AIC: Akaike Information Criteria; gEBV: Genomic estimated breeding value; S: Scenario; C: Cluster.

DECLARATIONS

Ethics approval and consent to participate

Not applicable.

Consent for publication

Not applicable.

Availability of data and materials

The datasets used and/or analyzed during the current study are available from the corresponding author on reasonable request.

Competing interests

The authors declare that they have no competing interests.

Funding

This work was supported by the China Agriculture Research System (CARS-36), the Program for Changjiang Scholar and Innovation Research Team in University (IRT_15R62), Beijing Sanyuan Breeding Technology Ltd Co. funded project (SYZYZ20190005), National Agricultural Genetic Improvement Program (2130135), Ningxia Agricultural Breeding Program (Dairy 2019NYYZ05), China Scholarship Council (No. 201913043). The funders had no role in study design, data collection and analysis, decision to publish, or preparation of the manuscript.

Authors' contributions

RS, LFB, YW designed the study. RS, LFB, AL, HL, ZC analyzed and interpreted data. RS wrote the manuscript. RS, LFB, AL, HM, BD, AVDL substantively revised the manuscript. LL, GG contributed to the access to tools and materials. All authors read and approved the final manuscript.

Acknowledgements

We would like to thank Shaolei Shi for management of genomic data, and Ganghui Dong, Xinyi Yan, Zezhao Wang, ZhiChao Zhang, Hetian Huang, Xiang Li, Qinglei Xu, Wei Xu, Jiangang Qi along with other CAU cattle genetics & breeding research

team members who participated in sample collection and provided helpful hints in discussion.

REFERENCES

1. Gonzalez-Recio O, Pérez-Cabal M, Alenda R. Economic Value of Female Fertility and its Relationship with Profit in Spanish Dairy Cattle. Journal of dairy science. 2004;87:3053–61.

2. Veerkamp RF, Beerda B. Genetics and genomics to improve fertility in high producing dairy cows. Theriogenology. 2007;68:S266–73.

3. Sun C, Madsen P, Lund M, Zhang Y, Nielsen U, Su G. Improvement in genetic evaluation of female fertility in dairy cattle using multiple-trait models including milk production traits. Journal of animal science. 2009;88:871–8.

4. Liu A, Lund MS, Wang Y, Guo G, Dong G, Madsen P, et al. Variance components and correlations of female fertility traits in Chinese Holstein population. J Animal Sci Biotechnol. 2017;8:56.

5. Falconer DS, Mackay TFC. Introduction to Quantitative Genetics. New York: Longman; 1996.

6. Liu A, Su G, Höglund J, Zhang Z, Thomasen J, Christiansen I, et al. Genotype by environment interaction for female fertility traits under conventional and organic production systems in Danish Holsteins. Journal of Dairy Science. 2019;102:8134–47.

7. Zhang Z, Kargo M, Liu A, Thomasen JR, Pan Y, Su G. Genotype-by-environment interaction of fertility traits in Danish Holstein cattle using a single-step genomic reaction norm model. Heredity. 2019;123:202–14.

8. Cheruiyot EK. Genotype-by-environment (temperature-humidity) interaction of milk production traits in Australian Holstein cattle. 2020;103:17.

9. Bohmanova J, Misztal I. Temperature-Humidity Indices as Indicators of Milk Production Losses due to Heat Stress. Journal of dairy science. 2007;90:1947–56.

10. Armstrong DV. Heat Stress Interaction with Shade and Cooling. Journal of Dairy Science. 1994;77:2044–50.

11. Ravagnolo O, Misztal I, Hoogenboom G. Genetic Component of Heat Stress in Dairy Cattle, Development of Heat Index Function. Journal of dairy science. 2000;83:2120–5.

12. Lambertz C, Sanker C, Gauly M. Climatic effects on milk production traits and somatic cell score in lactating Holstein-Friesian cows in different housing systems. Journal of dairy science. 2013;97:319-29.

13. West J, Mullinix B, Bernard J. Effects of Hot, Humid Weather on Milk Temperature, Dry Matter Intake, and Milk Yield of Lactating Dairy Cows. Journal of dairy science. 2003;86:232–42.

14. Cartmill JA, El-Zarkouny SZ, Hensley BA, Rozell TG, Smith JF, Stevenson JS. An Alternative AI Breeding Protocol for Dairy Cows Exposed to Elevated Ambient Temperatures before or after Calving or Both. Journal of Dairy Science. 2001;84:799–806.

15. Sammad A, Umer S, Shi R, Zhu H, Zhao X, Wang Y. Dairy cow reproduction under the influence of heat stress. Journal of Animal Physiology and Animal Nutrition. 2020;104:978–86.

16. Morton JM, Tranter WP, Mayer DG, Jonsson NN. Effects of Environmental Heat on Conception Rates in Lactating Dairy Cows: Critical Periods of Exposure. Journal of Dairy Science. 2007;90:2271–8.

17. Khan F, Prasad S, Gupta H. Effect of heat stress on pregnancy rates of crossbred dairy cattle in Terai region of Uttarakhand, India. Asian Pacific Journal of Reproduction. 2013;2:277–9.

18. Schüller LK, Burfeind O, Heuwieser W. Impact of heat stress on conception rate of dairy cows in the moderate climate considering different temperature–humidity index thresholds, periods relative to breeding, and heat load indices. Theriogenology. 2014;81:1050–7.

19. Misztal I, Legarra A, Aguilar I. Computing procedures for genetic evaluation including phenotypic, full pedigree, and genomic information. Journal of Dairy Science. 2009;92:4648–55.

20. Christensen OF, Lund MS. Genomic prediction when some animals are not genotyped. Genet Sel Evol. 2010;42:2.

21. Wang H, Misztal I, Aguilar I, Legarra A, Muir WM. Genome-wide association mapping including phenotypes from relatives without genotypes. Genet Res. 2012;94:73–83.

22. Akaike H. A New Look At The Statistical Model Identification. Automatic Control, IEEE Transactions on. 1975;19:716–23.

23. Berry DP, Wall E, Pryce JE. Genetics and genomics of reproductive performance in dairy and beef cattle. Animal. 2014;8:105–21.

24. Ghiasi H, Pakdel A, Nejati-Javaremi A, Mehrabani-Yeganeh H, Honarvar M, González-Recio O, et al. Genetic variance components for female fertility in Iranian Holstein cows. Livestock Science. 2011;139:277–80.

25. Berry DP, Kearney JF, Twomey K, Evans RD. Genetics of reproductive performance in seasonal calving dairy cattle production systems. Irish Journal of Agricultural and Food Research. 2013;52:1–16.

26. Liu J, Li L, Chen X, Lu Y, Wang D. Effects of heat stress on body temperature, milk production, and reproduction in dairy cows: a novel idea for monitoring and evaluation of heat stress — A review. Asian-Australas J Anim Sci. 2019;32:1332–9.

27. Wilson SJ, Kirby CJ, Koenigsfeld AT, Keisler DH, Lucy MC. Effects of Controlled Heat Stress on Ovarian Function of Dairy Cattle. 2. Heifers. Journal of Dairy Science. 1998;81:2132–8.

28. Sakatani M, Takahashi M, Takenouchi N. The efficiency of vaginal temperature measurement for detection of estrus in Japanese Black cows. Journal of Reproduction and Development. 2016;62:201–7.

29. Lozano Domínguez RR, Vásquez Peláez CG, Padilla EG. Effect of heat stress and its interaction with other management and productive variables on pregnancy rate in dairy cows in Aguascalientes, Mexico. Veterinaria Mexico. 2005;36:245-60.

30. Amundson JL, Mader TL, Rasby RJ, Hu QS. Environmental effects on pregnancy rate in beef cattle1. Journal of Animal Science. 2006;84:3415–20.

31. Morton JM, Tranter WP, Mayer DG, Jonsson NN. Effects of Environmental Heat on Conception Rates in Lactating Dairy Cows: Critical Periods of Exposure. Journal of Dairy Science. 2007;90:2271–8.

32. Silva FF, Mulder HA, Knol EF, Lopes MS, Guimarães SEF, Lopes PS, et al. Sire evaluation for total number born in pigs using a genomic reaction norms approach1. Journal of Animal Science. 2014;92:3825–34.

33. Ismael A, Strandberg E, Berglund B, Kargo M, Fogh A, Løvendahl P. Genotype by environment interaction for activity-based estrus traits in relation to production level for Danish Holstein. Journal of Dairy Science. 2016;99:9834–44.

34. Su G, Madsen P, Lund MS, Sorensen D, Korsgaard IR, Jensen J. Bayesian analysis of the linear reaction norm model with unknown covariates1. Journal of Animal Science. 2006;84:1651–7.

35. Santana ML, Eler JP, Cardoso FF, Albuquerque LG, Ferraz JBS. Phenotypic plasticity of composite beef cattle performance using reaction norms model with unknown covariate. Animal. 2013;7:202–10.

940 36. Kolmodin R, Strandberg E, Madsen P, Jensen J, Jorjani H. Genotype by
941 Environment Interaction in Nordic Dairy Cattle Studied Using Reaction Norms. Acta
942 Agriculturae Scandinavica, Section A - Animal Science. 2002;52:11–24.

943 37. Oliveira DP, Lourenco DAL, Tsuruta S, Misztal I, Santos DJA, de Araújo Neto
944 FR, et al. Reaction norm for yearling weight in beef cattle using single-step genomic
945 evaluation1. Journal of Animal Science. 2018;96:27–34.

946 38. Ilha GF, Rovani MT, Gasperin BG, Ferreira R, de Macedo MP, Neto OA, et al.
947 Regulation of Anti-Müllerian Hormone and Its Receptor Expression around Follicle
948 Deviation in Cattle. Reprod Domest Anim. 2016;51:188–94.

949 39. Poole DH, Ocón-Grove OM, Johnson AL. Anti-Müllerian hormone (AMH)
950 receptor type II expression and AMH activity in bovine granulosa cells.
951 Theriogenology. 2016;86:1353–60.

952 40. Hondo T, Kanaya T, Takakura I, Watanabe H, Takahashi Y, Nagasawa Y, et al.
953 Cytokeratin 18 is a specific marker of bovine intestinal M cell. Am J Physiol
954 Gastrointest Liver Physiol. 2011;300:G442-453.

955 41. Duncan A, Forcina J, Birt A, Townson D. Estrous cycle-dependent changes of Fas
956 expression in the bovine corpus luteum: influence of keratin 8/18 intermediate
957 filaments and cytokines. Reprod Biol Endocrinol. 2012;10:90.

958 42. Degrelle SA, Murthi P, Evain-Brion D, Fournier T, Hue I. Expression and
959 localization of DLX3, PPARG and SP1 in bovine trophoblast during binucleated
960 cell differentiation. Placenta. 2011;32:917–20.

961 43. Zhong J-L, Xu J-W, Wang J, Wen Y-F, Niu H, Zheng L, et al. A novel SNP of
962 PLAG1 gene and its association with growth traits in Chinese cattle. Gene.
963 2019;689:166–71.

964 44. Hou J, Qu K, Jia P, Hanif Q, Zhang J, Chen N, et al. A SNP in PLAG1 is
965 associated with body height trait in Chinese cattle. Anim Genet. 2020;51:87–90.

966 45. Mota LFM, Lopes FB, Fernandes Júnior GA, Rosa GJM, Magalhães AFB,
967 Carvalheiro R, et al. Genome-wide scan highlights the role of candidate genes on
968 phenotypic plasticity for age at first calving in Nellore heifers. Sci Rep.
969 2020;10:6481.

970 46. Huang Y-Z, Wang Q, Zhang C-L, Fang X-T, Song E-L, Chen H. Genetic Variants
971 in SDC3 Gene are Significantly Associated with Growth Traits in Two Chinese Beef
972 Cattle Breeds. Anim Biotechnol. 2016;27:190–8.

973 47. Liang W, Zhang HL, Liu Y, Lu BC, Liu X, Li Q, et al. Investigation of the
974 association of two candidate genes (H-FABP and PSMC1) with growth and carcass
975 traits in Qinchuan beef cattle from China. Genet Mol Res. 2014;13:1876–84.

48. Rudolf FO, Kadokawa H. Cytoplasmic kinases downstream of GPR30 suppress gonadotropin-releasing hormone (GnRH)-induced luteinizing hormone secretion from bovine anterior pituitary cells. J Reprod Dev. 2016;62:65–9.

49. Kujjo LL, Ronningen R, Ross P, Pereira RJG, Rodriguez R, Beyhan Z, et al. RAD51 plays a crucial role in halting cell death program induced by ionizing radiation in bovine oocytes. Biol Reprod. 2012;86:76.

50. Bilotto S, Boni R, Russo GL, Lioi MB. Meiosis progression and donor age affect expression profile of DNA repair genes in bovine oocytes. Zygote. 2015;23:11–8.

51. Ju Z, Zheng X, Huang J, Qi C, Zhang Y, Li J, et al. Functional characterization of genetic polymorphisms identified in the promoter region of the bovine PEPS gene. DNA Cell Biol. 2012;31:1038–45.

52. Pedersen LRL, Nielsen SB, Hansted JG, Petersen TE, Otzen DE, Sørensen ES. PP3 forms stable tetrameric structures through hydrophobic interactions via the C-terminal amphipathic helix and undergoes reversible thermal dissociation and denaturation. FEBS J. 2012;279:336–47.

53. Shin S, Heo J, Yeo J, Lee C, Chung E. Genetic association of phosphodiesterase 1B (PDE1B) with carcass traits in Korean cattle. Mol Biol Rep. 2012;39:4869–74.

54. Xu Y, Zhang L, Shi T, Zhou Y, Cai H, Lan X, et al. Copy number variations of MICAL-L2 shaping gene expression contribute to different phenotypes of cattle. Mamm Genome. 2013;24:508–16.

55. Dang Y, Li M, Yang M, Cao X, Lan X, Lei C, et al. Identification of bovine NPC1 gene cSNPs and their effects on body size traits of Qinchuan cattle. Gene. 2014;540:153–60.

56. Nemoto T, Toyoshima-Aoyama F, Ueda Y, Ohba T, Yanagita T, Watanabe H, et al. Involvement of the Orexin System in Adrenal Sympathetic Regulation. Pharmacology. 2013;91:250–8.

57. Doghman M, Delagrange P, Blondet A, Berthelon M-C, Durand P, Naville D, et al. Agouti-related protein antagonizes glucocorticoid production induced through melanocortin 4 receptor activation in bovine adrenal cells: a possible autocrine control. Endocrinology. 2004;145:541–7.

58. Doghman M, Delagrange P, Berthelon M-C, Durand P, Naville D, Bégeot M. Sustained inhibitory effect of Agouti Related Protein on the ACTH-induced cortisol production by bovine cultured adrenal cells. Regul Pept. 2005;124:215–9.

59. Tiwari RV, Parajuli P, Sylvester PW. [gamma]-Tocotrienol-induced endoplasmic reticulum stress and autophagy act concurrently to promote breast cancer cell death. Biochemistry and cell biology = Biochimie et biologie cellulaire. 2015;93:306.

60. White HM, Koser SL, Donkin SS. Regulation of bovine pyruvate carboxylase mRNA and promoter expression by thermal stress. J Anim Sci. 2012;90:2979–87.

61. Velez JC, Donkin SS. Feed restriction induces pyruvate carboxylase but not phosphoenolpyruvate carboxykinase in dairy cows. J Dairy Sci. 2005;88:2938–48.

62. Costa RB, Camargo GM, Diaz ID, Irano N, Dias MM, Carvalheiro R, et al. Genome-wide association study of reproductive traits in Nellore heifers using Bayesian inference. Genetics Selection Evolution. 2015;47:67.

63. Sakurai T, Bai H, Bai R, Sato D, Arai M, Okuda K, et al. Down-regulation of interferon tau gene transcription with a transcription factor, EOMES. Mol Reprod Dev. 2013;80:371–83.

64. Han B, Liang W, Liu L, Li Y, Sun D. Genetic association of the ACACB gene with milk yield and composition traits in dairy cattle. Anim Genet. 2018;49:169–77.

65. Taniguchi H, Komiyama J, Viger RS, Okuda K. The expression of the nuclear receptors NR5A1 and NR5A2 and transcription factor GATA6 correlates with steroidogenic gene expression in the bovine corpus luteum. Mol Reprod Dev. 2009;76:873–80.

66. Goravanahally MP, Sen A, Inskeep EK, Flores JA. PKC epsilon and an increase in intracellular calcium concentration are necessary for PGF2 alpha to inhibit LH-stimulated progesterone secretion in cultured bovine steroidogenic luteal cells. Reprod Biol Endocrinol. 2007;5:37.

67. Berisha B, Schams D, Rodler D, Sinowatz F. Expression pattern of HIF1alpha and vasohibins during follicle maturation and corpus luteum function in the bovine ovary. Reproduction in Domestic Animals. 2016; doi: 10.1111/rda.12867.

68. Sağsöz H, Ketani MA, Saruhan BG. Expression of the erbB/HER receptor family in the bovine uterus during the sexual cycle and the relation of this family to serum sex steroids. Biotech Histochem. 2012;87:105–16.

69. Wijayagunawardane MPB, Hambruch N, Haeger J-D, Pfarrer C. Effect of epidermal growth factor (EGF) on the phosphorylation of mitogen-activated protein kinase (MAPK) in the bovine oviduct in vitro: Alteration by heat stress. J Reprod Dev. 2015;61:383–9.

70. Nedvetsky PI, Meurer S, Opitz N, Nedvetskaya TY, Müller H, Schmidt HHHW. Heat shock protein 90 regulates stabilization rather than activation of soluble guanylate cyclase. FEBS Lett. 2008;582:327–31.

71. Sarkar A, Dai Y, Haque MM, Seeger F, Ghosh A, Garcin ED, et al. Heat Shock Protein 90 Associates with the Per-Arnt-Sim Domain of Heme-free Soluble Guanylate Cyclase: IMplications for Enzyme Maturation. J Biol Chem. 2015;290:21615–28.

72. Khan A, Dou J, Wang Y, Jiang X, Zahoor M, Hanpeng L, et al. Evaluation of heat stress effects on cellular and transcriptional adaptation of bovine granulosa cells. Journal of Animal Science and Biotechnology. 2020; doi: 10.1186/s40104-019-0408-8.

73. Browning BL, Zhou Y, Browning SR. A One-Penny Imputed Genome from Next-Generation Reference Panels. The American Journal of Human Genetics. 2018;103:338–48.

74. Yousef MK. Stress physiology in livestock. CRC Press; 1985.

75. Aguilar I, Misztal I, Johnson DL, Legarra A, Tsuruta S, Lawlor TJ. Hot topic: a unified approach to utilize phenotypic, full pedigree, and genomic information for genetic evaluation of Holstein final score. Journal of Dairy ence. 2010;93:743–52.

76. Gao H, Christensen OF, Madsen P, Nielsen US, Zhang Y, Lund MS, et al. Comparison on genomic predictions using three GBLUP methods and two single-step blending methods in the Nordic Holstein population. Genet Sel Evol. 2012;44:8.

77. VanRaden PM. Efficient Methods to Compute Genomic Predictions. Journal of Dairy Science. 2008;91:4414–23.

78. Powell JE, Visscher PM, Goddard ME. Reconciling the analysis of IBD and IBS in complex trait studies. Nature Reviews Genetics. 2010;11:800–5.

79. Vitezica ZG, Aguilar I, Misztal I, Legarra A. Bias in genomic predictions for populations under selection. Genet Res. 2011;93:357–66.

80. Misztal I. Complex Models, More Data: Simpler Programming? IEEE Internet Computing - INTERNET. 1999;20.

81. Su G, Lund MS, Sorensen D. Selection for litter size at day five to improve litter size at weaning and piglet survival rate1. Journal of Animal Science. 2007;85:1385–92.

82. Aguilar I, Misztal I, Tsuruta S, Legarra A, Wang H. PREGSF90 – POSTGSF90: Computational Tools for the Implementation of Single-step Genomic Selection and Genome-wide Association with Ungenotyped Individuals in BLUPF90 Programs. 2014; doi: 10.13140/2.1.4801.5045.

83. Thomas P, Campbell M, Kejariwal A, Mi H, Karlak B, Daverman R, et al. PANTHER: A Library of Protein Families and Subfamilies Indexed by Function. Genome research. 2003;13:2129–41.

84. Oliveira HR, Lourenco DAL, Masuda Y, Misztal I, Tsuruta S, Jamrozik J, et al. Single-step genome-wide association for longitudinal traits of Canadian Ayrshire, Holstein, and Jersey dairy cattle. Journal of Dairy Science. 2019;102:9995–10011.

1083

Figures

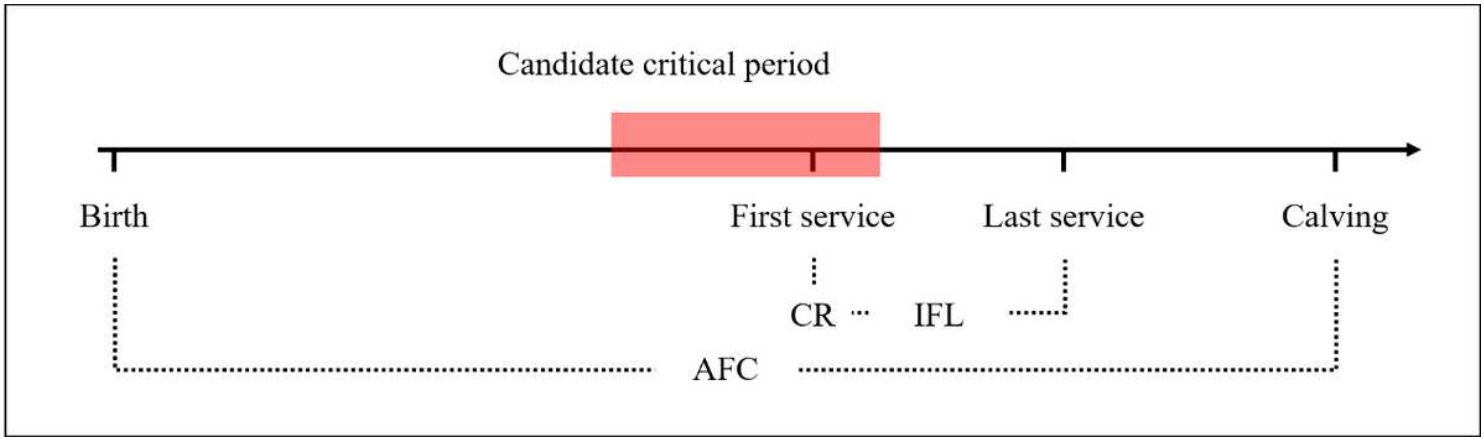

Figure 1

Reproductive events and the definition of critical period in heifers. The red rectangle represents the critical period, defining as the time period of which heifers are likely to suffer from heat stress. AFC = age at first calving, IFL = interval from first to last service, CR = conception rate of first service.

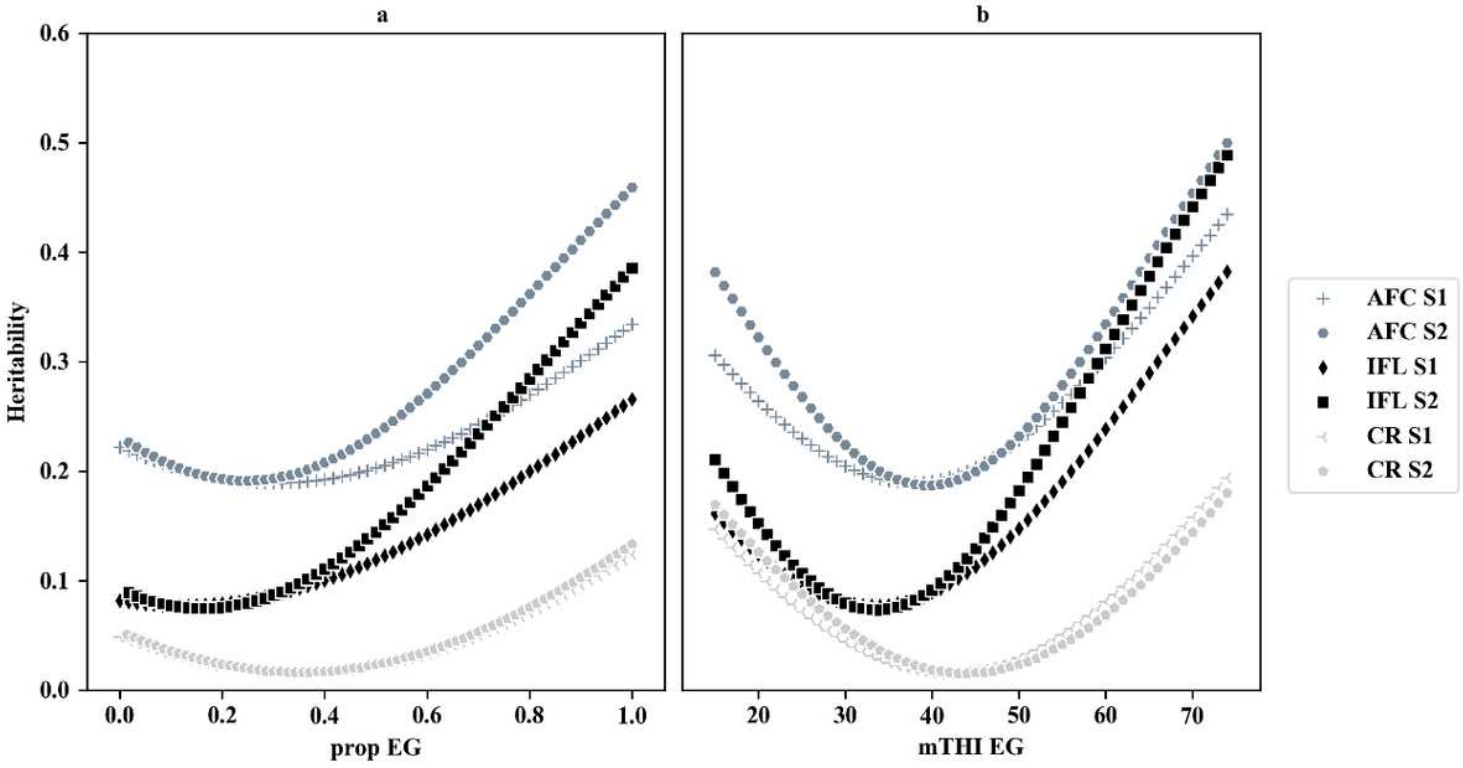

Figure 2

Heritabilities estimated by reaction norm models with the matrix H using a) prop-EG or b) mTHI-EG as environmental gradient. For a), the x-axis is the proportion of days exceeding the threshold with a range of 0 to 1; while for b), the x-axis is the minimum THI with a range of 15 to 75.

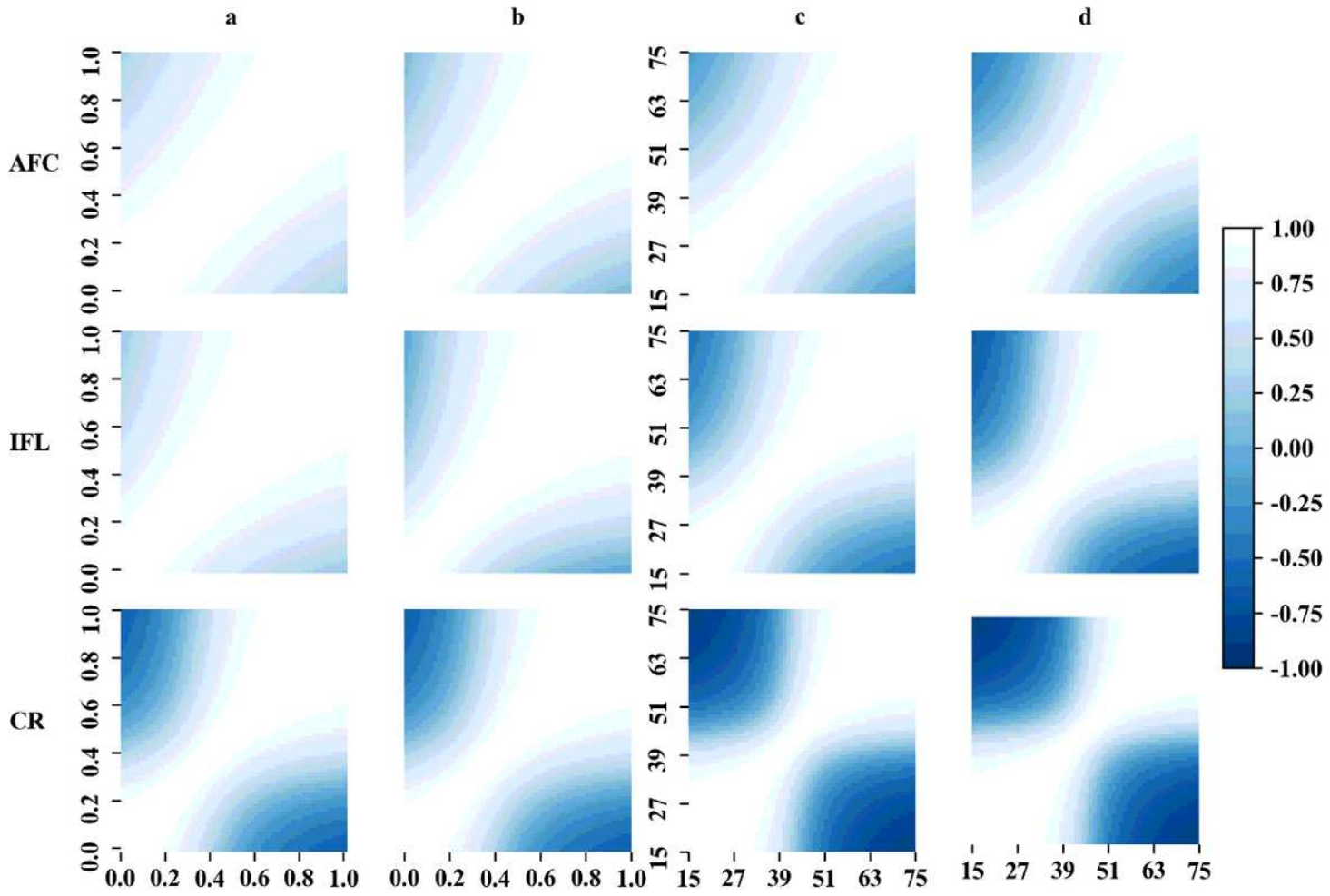

Figure 3

Genetic correlations estimated by reaction norm models (RNMs) with the matrix H. The color indicates the magnitude of the genetic correlation. a) Correlations between different levels of prop-EG estimated from RNM under S1. The x-axis and y-axis are the proportion of days exceeding the threshold, ranging from 0 to 1. b) Correlations between different levels of prop-EG estimated from RNM under S2. The x-axis and y-axis are the proportion of days exceeding the threshold, ranging from 0 to 1. c) Correlations between different levels of mTHI-EG estimated from RNM under S1. The x-axis and y-axis are the minimum THI, ranging from 15 to 75. d) Correlations between different levels of mTHI-EG estimated from RNM under S2. The x-axis and y-axis are the minimum THI, ranging from 15 to 75.

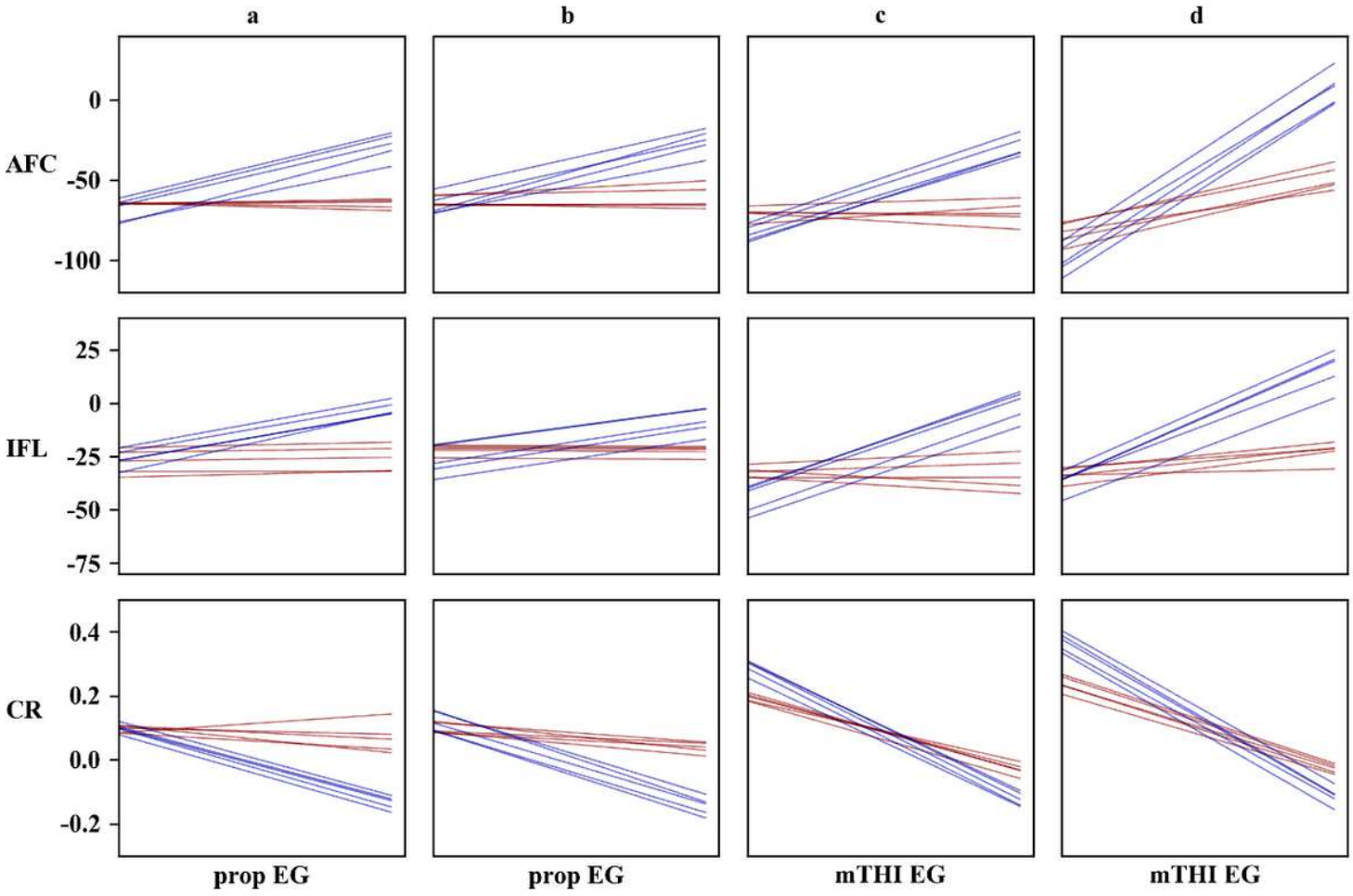

Figure 4

The re-ranking plots for gEBVs of sires. The blue and red lines represent sensitive and resilient sires, respectively. a) Re-ranking plots for three traits estimated using prop-EG under S1. The x-axis is the proportion of days exceeding the threshold with a range of 0 to 1 and y-axis is gEBV. b) Re-ranking plots for three traits estimated using prop-EG under S2. The x-axis is the proportion of days exceeding the threshold with a range of 0 to 1 and y-axis is gEBV. c) Re-ranking plots for three traits estimated using mTHI-EG under S1. The x-axis is the minimum THI with a range of 15 to 75 and y-axis is gEBV. d) Re-ranking plots for three traits estimated using mTHI-EG under S2. The x-axis is the minimum THI with a range of 15 to 75 and y-axis is gEBV

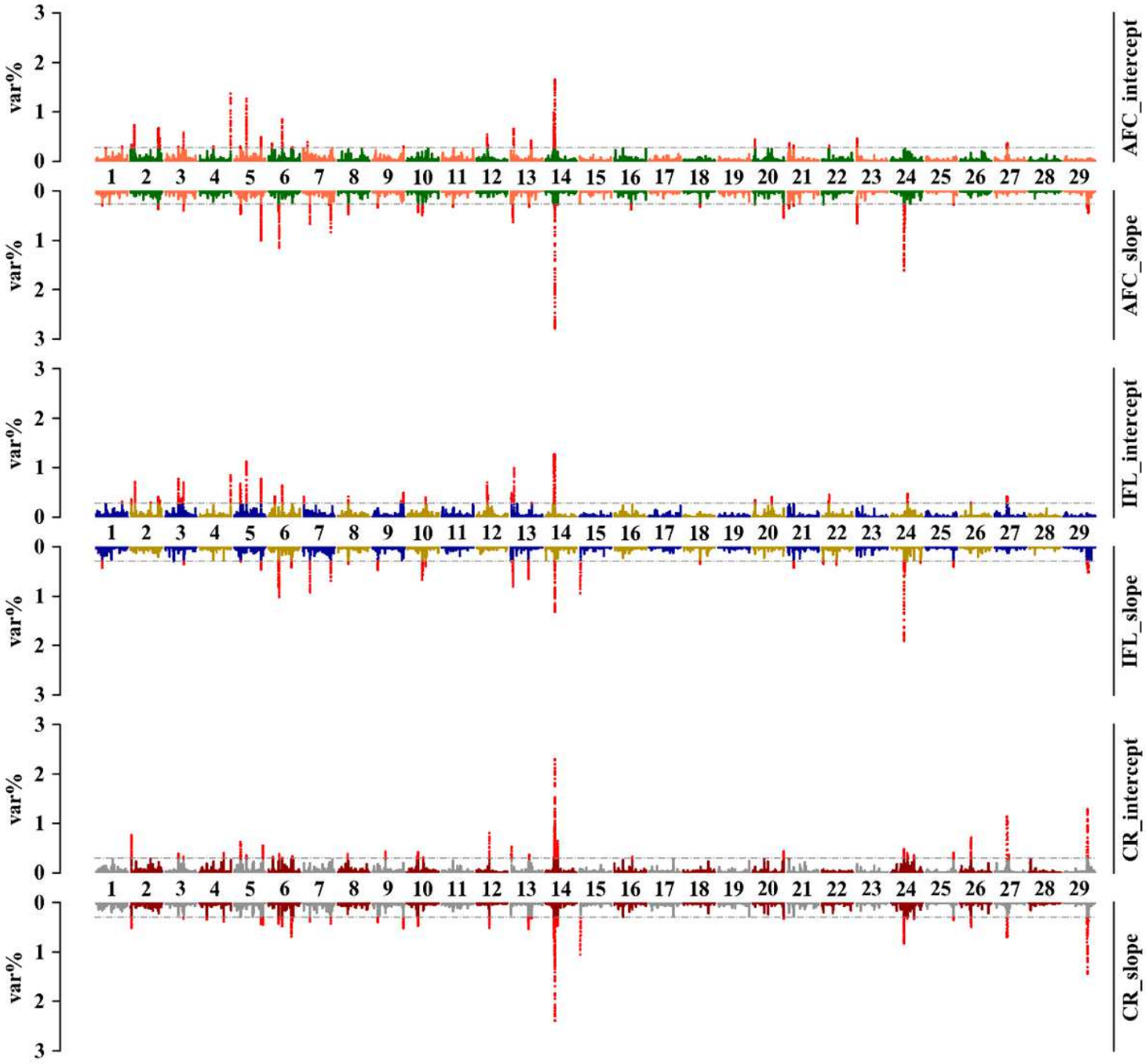

Figure 5

Percentages of the intercept and slope genetic variances explained by a sliding window of 20 SNPs for three traits, which were estimated under scenario one of prop-EG. The x-axis is autosome segments; the y-axis represents the proportion of explained variances; the grey horizontal lines are thresholds (top 0.5%) for candidate genomic regions; different color sets indicate different traits

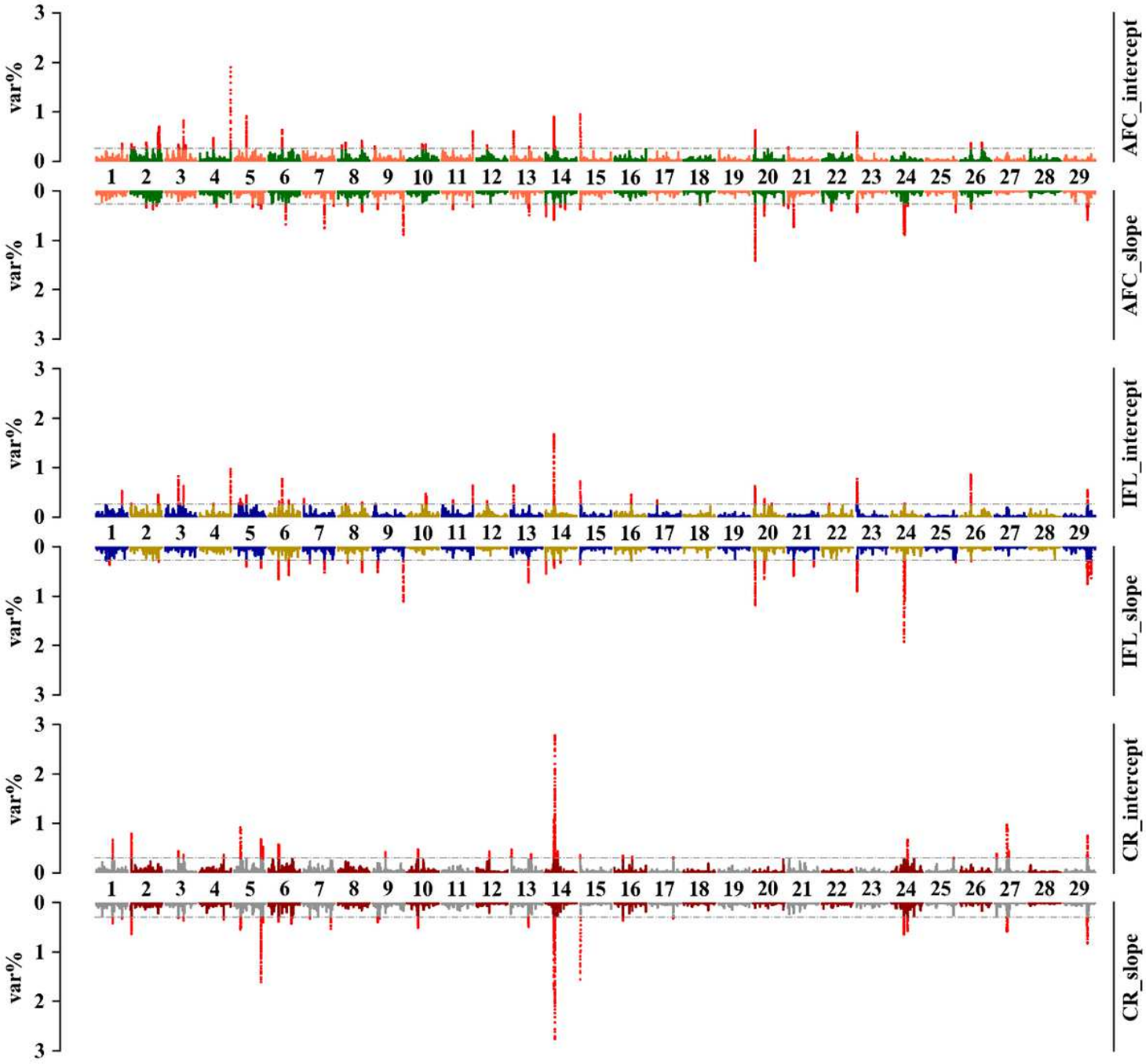

Figure 6

Percentages of the intercept and slope genetic variances explained by a sliding window of 20 SNPs for three traits, which were estimated under scenario two of prop-EG. The x-axis is autosome segments; the y-axis represents the proportion of explained variances; the grey horizontal lines are thresholds (top 0.5%) for candidate genomic regions; different color sets indicate different traits.

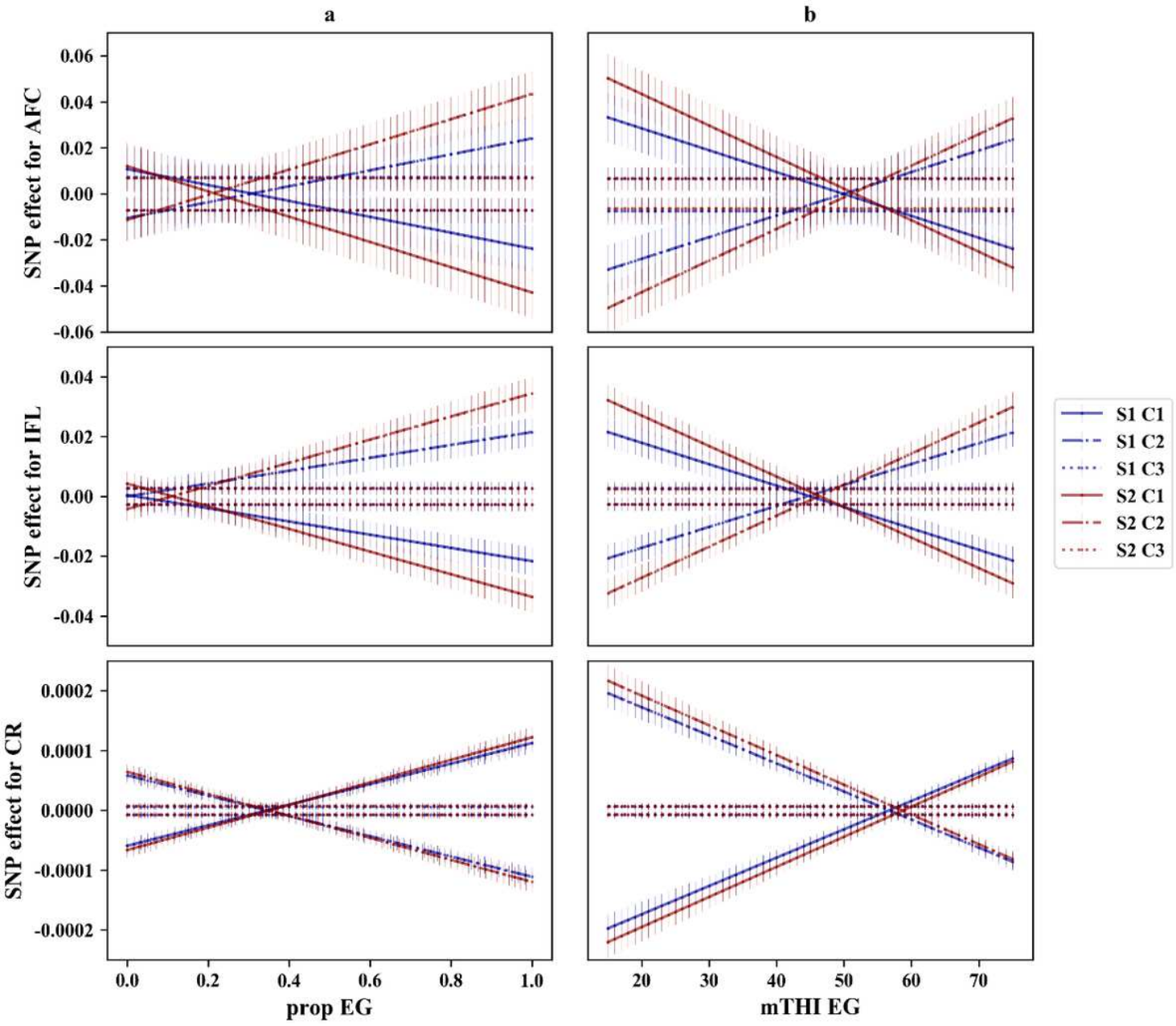

Figure 7

Trajectories of SNP effects changing over EGs. The x-axis is environmental gradient; the y-axis represents the SNP effects; vertical bar is the standard deviations of SNP effects at each level of EG; blue lines indicate scenario one; red lines indicate scenario two; different color sets indicate different clusters. a) Trajectories of SNP effects changing over prop-EG. The x-axis is the proportion of days exceeding the threshold with a range of 0 to 1. b) Trajectories of SNP effects changing over mTHI-EG. The x-axis is the minimum THI with a range of 15 to 75.

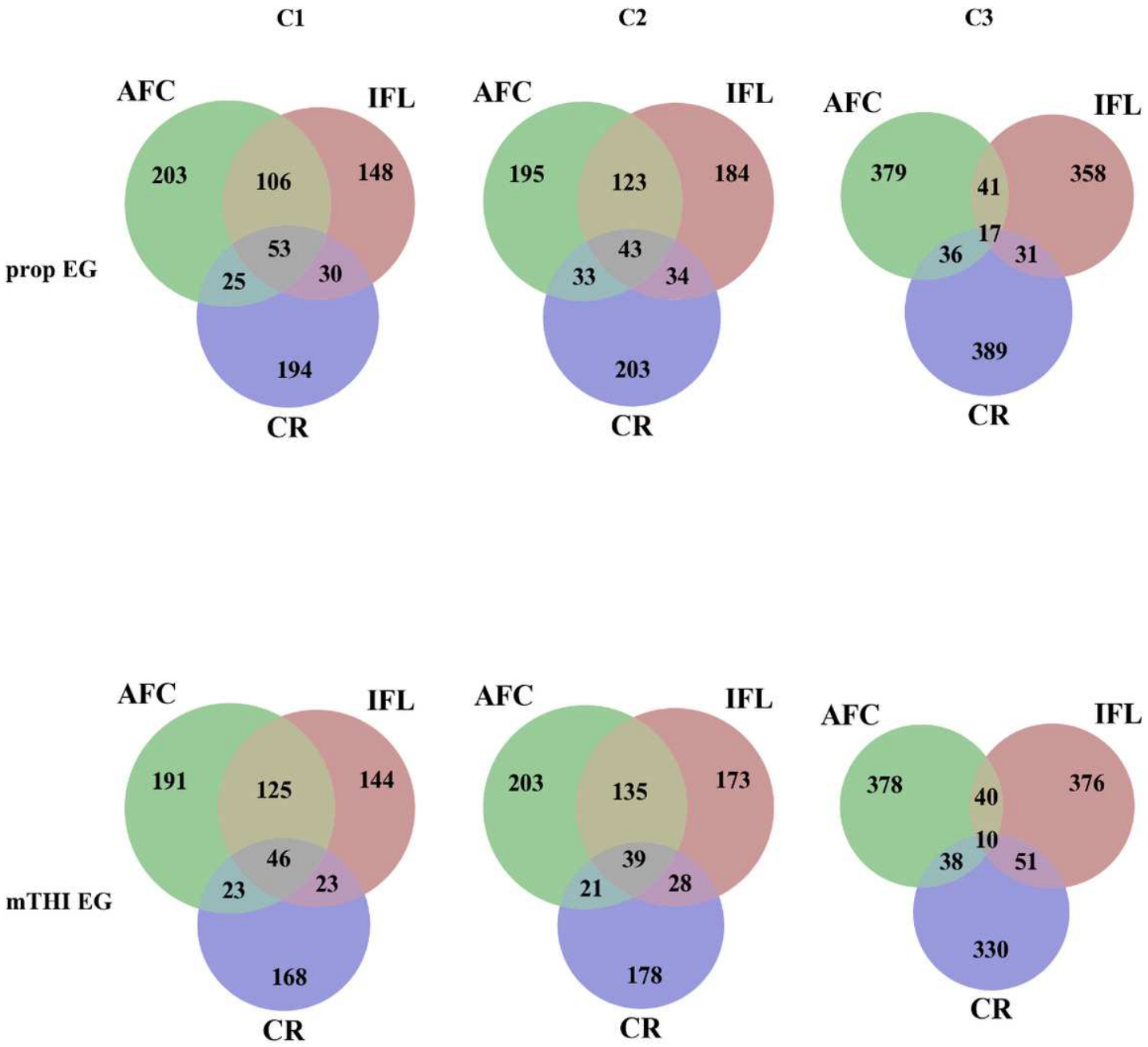

Figure 8

Number of shared candidate genes for each EG in different traits and clusters. C1 = SNP effects changes in preferential ways (decrease for AFC and IFL; increase for CR); C2 = SNP effects changes in the opposite ways (increase for AFC and IFL; decrease for CR); C3 = constant SNP effects over time.

Supplementary Files

This is a list of supplementary files associated with this preprint. Click to download.

- Supp.File1.jpg

- Supp.File2.xlsx
- Supp.File3.xlsx
- Supp.File4.xlsx
- Supp.File5.jpg
- Supp.File6.jpg
- Supp.File7.jpg
- Supp.File8.jpg
- Supp.File9.xlsx
- Supp.File10.xlsx
- Supp.File11.jpg